



EUROPEAN
COMMISSION

European
Research Area

Carbon-14 Source Term

CAST



3rd Annual WP3 Progress Report (D3.13)

Author(s):

Sophia NECIB, David BOTTOMLEY, Mohamed Ali BAHRI, Véronique BROUDIC, Crina BUCUR, Nadège CARON, Florence COCHIN, Frank DRUYTS, Manuela FULGER, Michel HERM, Viktor JOBBAGY, Laëtitia KASPRZAK, Solène LEGAND, Constantin Lorgulis, Volker METZ, Stéphane PERRIN, Tomofumi SAKURAGI, Tomo SUZUKI-MURESAN, Hiromi TANABE

Date of issue of this report: 19/09/2016

The project has received funding from the European Union's Seventh Framework Programme for research, technological development and demonstration under grant agreement no. 604779, the CAST project		
Dissemination Level		
PU	Public	X
RE	Restricted to the partners of the CAST project	
CO	Confidential, only for specific distribution list defined on this document	

CAST – Project Overview

The CAST project (CARbon-14 Source Term) aims to develop understanding of the potential release mechanisms of carbon-14 from radioactive waste materials under conditions relevant to waste packaging and disposal to underground geological disposal facilities. The project focuses on the release of carbon-14 as dissolved and gaseous species from irradiated metals (steels, Zircalloys), irradiated graphite and from ion-exchange materials.

The CAST consortium brings together 33 partners with a range of skills and competencies in the management of radioactive wastes containing carbon-14, geological disposal research, safety case development and experimental work on gas generation. The consortium consists of national waste management organisations, research institutes, universities and commercial organisations.

The objectives of the CAST project are to gain new scientific understanding of the rate of release of carbon-14 from the corrosion of irradiated steels and Zircalloys and from the leaching of ion-exchange resins and irradiated graphites under geological disposal conditions, its speciation and how these relate to carbon-14 inventory and aqueous conditions. These results will be evaluated in the context of national safety assessments and disseminated to interested stakeholders. The new understanding should be of relevance to national safety assessment stakeholders and will also provide an opportunity for training for early career researchers.

For more information, please visit the CAST website at:

<http://www.projectcast.eu>

CAST		
Work Package: 3	CAST Document no. :	Document type:
Task: 3.3	CAST-2016-D3.13	R = report
Issued by: Andra		Document status:
Internal no. DRPFSCM160035		Final

Document title
3 rd Annual WP3 Progress Report

Executive Summary

Work Package 3 (WP3) is related to Zircaloy in the CAST project. It aims to better understand C-14 behaviour in waste Zr fuel claddings under disposal conditions with regard to C-14 inventory (and origins), release from waste packages and speciation of released C-14. In order to achieve these objectives, WP3 has been divided into four tasks (from 3.1 to 3.4) and 20 deliverables (from D3.1 to D3.20).

Tasks 3.1 and 3.2 are completed and were devoted to the State of the Art review and analytical development respectively. Task 3.3 is ongoing and aims to characterise the C-14 inventory and C-14 release from leaching experiments and corrosion experiments in alkaline media representative of disposal conditions. Finally, Task 3.4 will summarise and synthesise the work performed during the previous Tasks.

During the third year of the CAST project, WP3 participants have essentially worked on Task 3.2. In total 3 deliverables, including this one, have been submitted to the coordinator of the CAST project for review. For Task 3.2, deliverable D3.9 was submitted after a 9 month delay. It presents the quantification of C-14 in liquid and gas.

Overall, the analytical strategy has highlighted the possible analytical techniques to measure C-14 inventory and speciation. LSC (Liquid Scintillation Counting) is used to determine carbon mass balance from solution sampled after 14 days onwards. AMS (Accelerated Mass Spectrometry) is foreseen to quantify C-14 inorganic and organic molecules.

To determine the speciation of organic molecules, spectroscopic methods such as Infra-red have been used to identify the main families of chemical functions (carboxylic acids, aromatic compounds, ketones, alcohols etc...). Chromatographic techniques have been used to detect and quantify families of molecules with low mass molecules. Electrospray – mass spectrometry analysis (ESI-MS) will be attempted by CEA to detect the molecules with higher molecular weight. Gas chromatography (GC) is also foreseen by SCK.CEN to determine C-14 speciation in Ca(OH)₂ solution.

Some groups (KIT, and RWMC) have performed gas analyses by using gas chromatography.

For Task 3.3, WP3 participants have run leaching tests in an acidic medium (for C-14 inventory purposes) as well as in alkaline medium (repository pH conditions). Deliverable D3.12 describes the work on corrosion performed in 2016.

Corrosion experiments will be performed on both, non-irradiated and irradiated Zr, in the reference solution or in Ca(OH)₂. Electrochemical measurements (Linear Polarisation Resistance (LPR) and hydrogen measurement techniques have been carried out to measure the corrosion rates of irradiated and unirradiated Zircaloy. A technique involving Co-60 gamma counting of the leaching solution will also be experimented to estimate the corrosion rate of Zircaloy.

- JRC/ITU intends to launch leaching experiment on irradiated Zircaloy in an autoclave filled with a solution of NaOH (pH 12) at different temperatures up to 80°C. The corrosion rate will be measured as well as C-14 quantified (gas + liquid)
- RATEN ICN has started the leaching experiment on irradiated Zircaloy -4. The first sample has been taken after 6 months of exposure. Corrosion rate measurements will be conducted by using electrochemical techniques. C-14 (total + inorganic / organic partition) will be measured by LSC.
- RWMC performed corrosion rate measurements by the gas ampoule method on unirradiated zirconium exposed to pure water at 30, 50 and 80°C for 1.5 years.

- SCK.CEN has launched preliminary polarisation measurements were conducted to study the electrochemical behaviour of the material.

The role of zirconia and its part in the instant release fraction is being investigated. It seems that considering zirconia as IRF only is too conservative according to:

- the low corrosion rate of zirconium
- the C-14 activity in the metal and zirconia
- the released rate of C-14 in alkaline media

List of Contents

Executive Summary	i
List of Contents	v
1 Introduction	7
2 Progress	7
2.1 Andra	7
2.2 Armines/Subatech contribution in WP3	8
2.2.1 Analytical strategy: principle	8
2.2.2 Radiochemical composition of the irradiated Zircaloy leaching solution	10
2.2.3 Leaching solution treatments	11
2.2.3.1 Removal of cesium	11
2.2.3.2 Removal of cobalt, nickel, iron, chromium and manganese	12
2.2.3.3 Removal of antimony	13
2.2.4 Leaching solution from irradiated Zircaloy hulls	14
2.2.4.1 Decontamination using $K_2[CuFe(CN)_6]$ without binder polymer	14
2.2.5 Ion chromatography of the decontaminated leachate	16
2.2.6 Quantification of C-14 carboxylic acids in the decontaminated leachate by LSC	17
2.3 CEA contribution in WP3	18
2.3.1 Materials Characterisations	18
2.3.2 Leaching experiments	20
2.3.2.1 Preliminary test	20
2.3.2.2 Leaching test	21
2.3.3 Analytical strategy	22
2.3.3.1 Carbon mass balance	22
Total organic and inorganic carbon	22
Total ^{14}C determination	23
Organic and inorganic ^{14}C partition	23
2.3.4 Speciation	25
2.3.5 Conclusions	27
2.4 ITU / JRC contribution in WP3	28
2.4.1 Non irradiated materials	28
2.4.2 Modelling	30
2.4.3 Leaching test	30
2.4.3.1 Samples	30
2.4.3.2 Autoclaves for leaching tests	31
2.4.4 C-14 analyses	32
2.4.4.1 Glove box	32
2.4.4.2 Total carbon content measurements	34
2.4.5 Overall schedule	35
2.5 KIT contribution in WP3	35
2.5.1 Introduction	35
2.5.2 Improvement of the separation technique	36
2.5.3 Inventory and chemical form of C-14	37
2.5.4 Summary and conclusions regarding the inventory and chemical form of C-14 in Zircaloy-4	40

2.6	RATEN ICN contribution in WP3	41
2.6.1	Leaching tests on irradiated Zy-4 samples	41
2.6.2	Modelling the C-14 accumulation in CANDU Zy-4 tube during fuel irradiation	45
2.7	RWMC contribution in WP3	50
2.7.1	Distribution of ¹⁴ C in irradiated cladding	50
2.7.2	Released ¹⁴ C from irradiated cladding	52
2.7.3	Acknowledgement	57
2.8	SCK.CEN contribution in WP3	58
2.8.1	Materials	58
2.8.2	Corrosion test	63
2.8.2.1	Static tests	63
2.8.2.2	Polarised corrosion tests	64
2.8.3	Gas chromatography	65
3	Summary	66
3.1	Introduction	66
3.2	Task 3.1	67
3.1	Tasks 3.2 and 3.3	68
3.1.1	Materials	68
3.1.2	Task 3.2	73
3.1.3	Task 3.3	75
4	Conclusions and perspectives	83
	References	84

1 Introduction

Work Package 3 (WP3) is related to Zircaloy in the CAST project. It aims to obtain a better understanding of C-14 behaviour in waste Zr fuel claddings under disposal conditions with regard to C-14 inventory (and origins), release from waste packages and speciation of released C-14. In order to achieve these objectives, WP3 has been divided into four tasks (from 3.1 to 3.4) and 20 deliverables (from D3.1 to D3.20).

Task 3.1 has been completed and was devoted to reviewing and establishing the current State of the Art on the C-14 release from zirconium alloy fuel claddings. Task 3.2 is devoted to developing analytical methods for the characterisation of C-14 organic and inorganic molecules. Task 3.3 is devoted to characterising the C-14 inventory and C-14 release from irradiated zirconium alloy fuel claddings sampled from different BWRs and PWRs. This is being determined from corrosion of activated materials (Zircaloy-2 (Zr2), Zircaloy-4 (Zr4) and Zircaloy M5™) in experiments under conditions relevant to deep geological disposal (cementitious/argillaceous media, aerobic/anaerobic). Acid dissolution of irradiated hulls has been used to measure total amounts of C-14. Finally, Task 3.4 will synthesise the work undertaken in the other tasks into a final report, to develop an interpretation of C-14 behaviour in zirconium alloy fuel claddings (C-14 inventories, release rates and speciation of released C-14) under disposal conditions.

This annual report summarises the work undertaken during the 3rd year of the CAST Project by all the organisations involved in WP3; Andra, Areva, Armines/Subatech, CEA, ITU/JRC, KIT, RATEN ICN, RWMC and SCK/CEN. It focuses mainly on Tasks 3.2 and 3.3.

2 Progress

This section describes the contributions from July 2015 to July 2016 for each participant involved in WP3.

2.1 Andra

Andra is in charge of coordinating WP3. This also involves the production of five deliverables over a period of four years (2014-2017): D3.1 (issued in 2014); D3.5 (issued in

2014); D3.11 (issued in 2015); D3.13 (due in 2016) and D3.20 (due in 2017). A joint progress meeting with WP2 of CAST was organised and held on 1 and 2 June 2016.

Overall, the third year was dedicated to discuss and clarify the following points:

- The experimental set-up for the leaching experiments on irradiated Zircalloys
- The reference time for the leaching experiments
- The analytical strategy including the use of AMS
- The techniques to measure the corrosion rate (CR) of Zr
- The first results obtained on C-14 measurements (inventory + speciation)
- The role of zirconia in C-14 release (IRF, dissolution rate)

2.2 Armines/Subatech contribution in WP3

During the 3rd year of the CAST project, Armines / Subatech was in charge of D3.9 in Task 3.2 entitled “Quantification of C-14 in liquid and gas phases”. It consists of describing the analytical method foreseen to analyse the organic carbon compounds released from irradiated materials containing ¹⁴C. The deliverable was submitted in June 2016 after a 9 month delay due to ongoing development of a strategy to analyse the small organic acids in contaminated solutions (see D3.9 report).

In WP3, Armines / Subatech works in collaboration with CEA Marcoule for the leaching experiment and shipment of solution, as well as CEA-LASE and CEA-LRMO for the speciation and quantification of C-14 in solution. Gas analysis was supposed to be developed by Subatech based on the availability of the gas samples from the leaching experiments run by CEA. During the first year of the CAST project, discussions with the laboratories involved Task 3.2, as well as during the second technical meeting in Brussels, it was agreed that gas sampling would be difficult to operate and therefore any gas samples would not be collected. Subatech/ARMINES needed to face to another difficulty which was to decontaminate a radioactive leaching solution without modifying carboxylic acids to send at the final stage to an AMS for analysis.

2.2.1 Analytical strategy: principle

The proposed strategy aims to detect and quantify low molecular weight organic compounds released with extremely low concentrations, in presence with other radionuclides such as

activated products, fission products and actinides. Characterization of carboxylic acids with low carbon chain length is of importance since they are preferentially released compounds from Zircaloy alloys and steels [SASOH, 2008; TAKAHASHI, 2013; HEIKOLA, 2014]. Such characterizations will be performed thanks to the combination of Ion Chromatography (IC) and Liquid Scintillation Counting (LSC). The IC technique will be used for the separation and fractionation of the carboxylic acids present in the leachates. However, this technique is not sensitive enough to quantify the very low concentrations of small carboxylic acids expected in the leaching solution. Therefore, collected carboxylic acids fractions will be transferred to the LSC device for the quantification of carbon-14 activity. LSC is a sensitive analytical technique (DL 0.04 Bq/mL). For extremely low activity level of leached C-14 in the collected fractions, below the detection limit of the LSC technique, accelerator mass spectrometry (AMS) is being considered with an external laboratory in CEA Saclay.

A second major objective developed at Armines/Subatech is to implement one simple and adapted method for the extraction of the main water soluble radionuclides other than C-14 in the leaching solution by using ion exchange resins (IER). The resin treatment stage has several goals:

- i) to reduce the total activity in leachates to avoid further dilution of the leaching solutions to meet the activity acceptance limits of the analytical laboratories and to make handling the leachates easier;
- ii) to limit the contamination of analytical equipment, especially for AMS analyses where institutions equipped with AMS cannot accept 'hot' samples;
- iii) to remove beta emitter radionuclides which interfere with the measurement of C-14 activity by LSC. Indeed, some soluble radionuclides are negatively charged in the hydroxides or oxo-anions forms and thus may appear in the collected fractions preventing an accurate quantification of C-14 using LSC.

The developed extraction method based on IER meets two essential criteria:

(1) minimization of the number of treatment stages inducing a loss of C-14 and (2) no alteration of C-14 target molecules. Figure 1 shows the overview of this strategy.

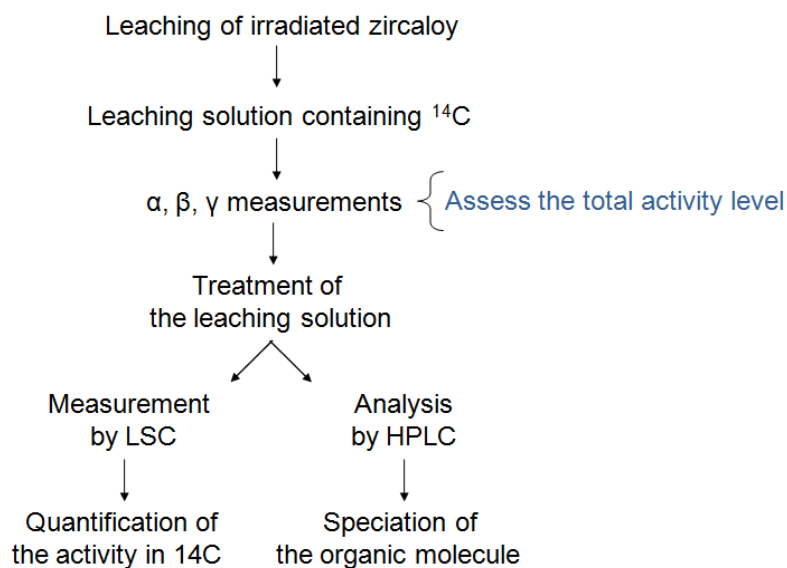


Figure 1: analytical strategy for the speciation of carbon-14 in solution.

2.2.2 Radiochemical composition of the irradiated Zircaloy leaching solution

The method for the extraction of main water soluble radionuclides in the leachates developed at SUBATECH took into account most reported radionuclides from the leaching of irradiated Zircaloy. Leaching experiments at RWMC on irradiated Zircaloy-2 from BWR cladding show a substantial presence of Co-60 in addition to Cs-137 and Sb-125 [JOBAGY, 2014]. Yamaguchi et al [YAMAGUCHI, 1999] reported the presence of Co-60, Cs-134, Cs-137, Eu-154, Ru-106, Rh-106 and Sb-125 in the leachates of Zircaloy-4 cladding from a PWR. The analyses performed on leachates from the leaching experiment carried out by CEA Marcoule on M5-type (UOX) Zircaloy hulls in NaOH, revealed a high activity mainly related to Sb-125, Cs-137 and Ru-106/Rh-106. Radiochemical analysis detected also minor activities from the presence of Cs-134, and Cr-51. The results are reported in Table 1 and details on the experimental conditions and characteristics of the used Zircaloy cladding are presented in the D3.2 report [CARON, 2014].

Table 1: Radiochemical composition (Bq/mL) of the leaching solution of M5-type (UOX) Zircaloy cladding in NaOH pH 12 solution, sampled at 14 days, PTFE 0.45 µm Filtration. (DTCD/SECM/LMPA laboratory).

alpha counting Total activity (Bq/mL) accuracy	59 24
beta counting Total activity (Bq/mL) accuracy	2300 115
gamma spectrometry Total activity (Bq/mL) ¹³⁴ Cs ¹³⁷ Cs ¹²⁵ Sb ²⁴¹ Am ¹⁰⁶ Ru/ ¹⁰⁶ Rh ⁶⁰ Co ¹⁵⁵ Eu ¹⁵⁴ Eu ⁵¹ Cr	2430 30 996 691 12 659 5,1 <0,5 6,4 33

2.2.3 Leaching solution treatments

2.2.3.1 Removal of cesium

The cesium removal can be ensured by using inorganic ion exchangers such as potassium hexacyanocobalt(II) ferrate(II), potassium hexacyanonickel(II) ferrate(II) and potassium hexacyanocopper(II) ferrate(II). These are good candidates for a rapid and quantitative fixation of cesium, stable for the entire pH range, efficient for any pH value ranging from acidic to alkaline conditions, radiation resistant and have weak interaction with nonmetallic ions [COLLINS, 1995; MIMURA, 1997; KAMENIK, 2012].

In this work, commercial potassium hexacyanocopper(II) ferrate(II) $K_2[CuFe(CN)_6]$ (KCFC) was tested for radionuclides extraction tests. An organic binding polymer based on polyacrylonitrile is added to the active component to improve its mechanical and granulometric properties. Nevertheless, the free residual cyano groups of the polymer support are reactive towards carboxylic groups and lead to a significant loss of the target carboxylic acids in the leaching solution. Thus, $K_2[CuFe(CN)_6]$ without binding polymer supplied by Areva STMI is considered in the experiments. The sorption measurements were made in batch equilibration tests containing 100 Bq of Cs-137. A large excess of resin (1 g

of dry resin) was added into the sample containing 100 Bq of Cs-137 in 20 mL of milliQ water. The remaining activity in the solution after contact with the ion exchanger was measured by LSC. The same experiment was reproduced with C-14 labelled short chain mono- and di-carboxylic acids to verify the absence of interaction with KCFC. Table 2 summarizes the recovery of Cs-137 and C-14 labelled carboxylic acids after contact for one hour. These results validate the quantitative removal of cesium and the selectivity of KCFC to allow the separation of caesium from small carboxylic acids.

Table 2: Recovery of Cs-137 and C-14 labelled carboxylic acids after 1 hour in contact with KCFC resin. The initial activity was 100 Bq.

Radionuclides	% Recovery
Cs-137	1%
C-14 formate	100%
C-14 propanoate	99.5%
C-14 butyrate	100%
C-14 oxalate	96%

2.2.3.2 Removal of cobalt, nickel, iron, chromium and manganese

Chelex 100 resin has a strong retention of multivalent transition metals and is usually used for the removal of trace metal contaminants in natural waters. It is stable over a wide pH range, weakly interacts with organic anions, is radiation resistant and is used for extraction and pre-concentration of radionuclides [PAI, 1988-a; PAI, 1988-b; BIORAD; ALLIOT, 2013; PAKALNS, 1980].

When it is in sodium form, Chelex 100 acts as a cation exchanger and allows the removal of polyvalent transition metals [PAI, 1988-a; PAI-b, 1988], and more specifically Co, Ni, Fe, Cr and Mn, from solution. Unlike KCFC, Chelex 100 efficiency is strongly pH dependent, the equilibrium pH value of the system affects greatly the fixation of polyvalent transition metals [PAI, 1988-b]. In this work, the pH value of the leaching solution, initially equal to 12, has to be adjusted to neutral pH to ensure free metal cations and avoid hydroxide complexes that cannot enter the pore structure of the resin [PAI, 1988-a]. At this neutral pH, carboxylic acids remain ionized as the pH is higher than their pKa (mostly lower than 5).

Chelex 100 (Analytical Grade Chelex 100 Resin, 50-100 mesh, supplied by Biorad) tests were made using a batch method. A solution of 30 mL containing radionuclides (Co-60, Ni-

63 and C-14) was put in contact with 1 g of Chelex 100 under agitation for at least 24 hours. After centrifugation, the supernatant was recovered and the remaining radionuclide activity of quantified by LSC. The measurements summarized in Table 3 confirm the high efficiency of Co-60 and Ni-63 removal with Chelex 100 and the absence of significant interaction with C-14 labelled carboxylic acids.

Table 3: Recovery of Co-60, Ni-63 and C-14 labelled carboxylic acids after 24 hours in contact with Chelex 100 resin. The initial activity was 100 Bq.

Radionuclides	% Recovery
Co-60	5%
Ni-63	3%
C-14 formate	100%
C-14 propanoate	93%
C-14 butyrate	98%
C-14 oxalate	98%

2.2.3.3 Removal of antimony

To remove antimony, Chelex 100 needs to be used in the ferric form. According to Chanda and al. [CHANDA, 1988], oxoanion species of arsenic (III) and (V) are efficiently removed from aqueous solution by ligand sorption on Chelex-Fe(III) complex. Due to similarities in the coordinating properties between arsenic and antimony, one could expect an efficient removal of antimony using Chelex 100 doped with Fe(III) cations. Under oxic conditions and in diluted solutions, SbO_3^- is the main species present in alkaline conditions [FILELLA, 2002; PITMAN, 1957; TAKENO, 2005; FILELLA, 2003].

To optimize the pH for Sb(V) retention with Chelex-Fe(III), a solution of Sb(V) was made by oxidizing SbCl_3 in presence of goethite as a catalyst. Isotherm sorption experiments were performed from pH 5 to 12. From Figure 2, there is an effective retention of Sb(V) when pH is between 5 and 6. Above these values, the retention of Sb(V) on Chelex-Fe(III) drops drastically since Chelex-Fe(III) decomposes at high pH values and forms hydroxide complexes. C-14 labelled carboxylic acids were contacted with Chelex-Fe(III) at pH 6 to determine any interaction with the target molecules. The obtained values of retention rate are represented in Table 4. A significant retention activity of carboxylic acids with Chelex-

Fe(III) at up to 91% for oxalate is observed, which prevents the use of Chelex-Fe(III) for the decontamination of antimony from the leaching solution.

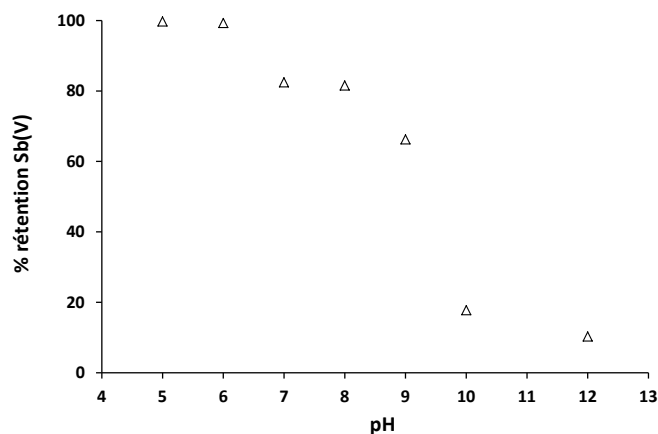


Figure 2: Retention variation of Sb(V) at different pH ranging from 5 to 12

Table 4 Retention of carboxylic acids with Chelex-Fe(III) at pH 6.

Carboxylic acids	% retention
Formate	4
Propanoate	25
Butyrate	48
Oxalate	91
Sb(V)	> 99

2.2.4 Leaching solution from irradiated Zircaloy hulls

2.2.4.1 Decontamination using $K_2[CuFe(CN)_6]$ without binder polymer

After 14 days of leaching experiments on irradiated Zircaloy M5TM, CEA-Marcoule shipped leachate solution filtered through a PTFE membrane filter (pore size 0.45 μ m). The solution was decontaminated by the resin $K_2[CuFe(CN)_6]$ without binder polymer due to its short time to reach equilibrium (one hour) and for its capacity to decontaminate several radionuclides encountered in the leaching solution. For optimal sorption on resin, the pH of the leaching solution, initially equal to 12, was reduced to pH 9 by adding HCl. Table 5 summarizes the activities measured before and after the decontamination of the leachate.

Table 5 Radiochemical composition of the leaching solution of M5-type (UOX) Zircaloy cladding before and after contact with $K_2[CuFe(CN)_6]$. Activity unit: Becquerels per mL.

	Activities in the leaching solution before $K_2[CuFe(CN)_6]$ contact	Activities in the leaching solution after $K_2[CuFe(CN)_6]$ contact
alpha counting		
Total activity	59	0.07
accuracy	24	0.03
beta counting		
Total activity	2300	50
accuracy	115	4
gamma spectrometry		
Total activity	2430	
^{134}Cs	30	< LD (0.2)
^{137}Cs	996	2.1
^{125}Sb	691	54.7
^{241}Am	12	< LD (0.1)
^{106}Ru - ^{106}Rh	659	3.4
^{60}Co	5.1	< LD (0.2)
^{155}Eu	<0,5	< LD (0.2)
^{154}Eu	6.4	< LD (0.2)
^{51}Cr	33	0.4

After contact with $K_2[CuFe(CN)_6]$, effective removal of actinides was performed as evidenced by a marked decrease of the total alpha activity. Likewise, total beta activity was considerably lowered to reach 50 Bq/mL. For gamma emitters initially present in the

leaching solution, most noteworthy was the remaining activity due to Sb-125 and Ru-106/Rh-106 which were substantially decreased compared to their activities before contact with $K_2[CuFe(CN)_6]$.

After decontamination of the leachate, ion chromatography was used for the separation and fractionation of the anionic carboxylic acids present in the leachates.

2.2.5 Ion chromatography of the decontaminated leachate

Decontaminated leachate was injected into the chromatographic device with the following characteristics: eluent/mobile phase Na_2CO_3 (7.5 mM) and NaOH (0.75 mM), suppressed conductivity detection, separation column Metrosep Asupp 16 250-2.0, injected volume 250 μ l, pump flow maintained at 0.15 mL/min to maximize the separation peaks. To analyse C-14 related to 1 mL of the leachate, fractionation of the decontaminated leachates was repeated four times and the carboxylic acids were collected separately based on the retention time of the carboxylic acids standards. Figure 3 shows the chromatograms of the decontaminated leachate and the mixture of carboxylic acids standards. The presence of the Cl peak is due to the acidification process with HCl. The fraction collection was performed over five minutes to ensure a full coverage of the carboxylic acids contained in the leachate. For the analysis of C-14 activity in the collected fractions, two peaks were selected: oxalate and butyrate with a total collected volume equal to 3 mL. C-14 quantification was performed with LSC.

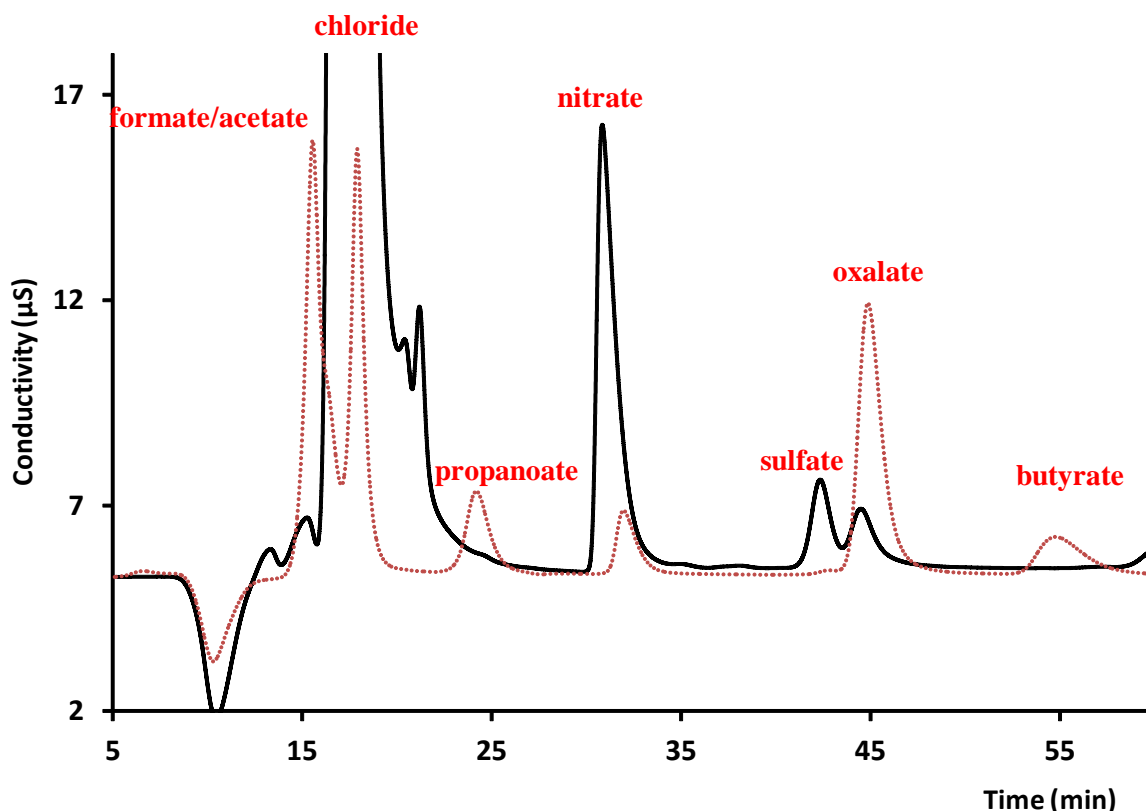


Figure 3 Chromatograms of the decontaminated leachate (solid line) and mixture of carboxylic acids (dotted line). Mobile phase: Na_2CO_3 (7.5 mM) and NaOH (0.75 mM). Injected volume 250 μL .

2.2.6 Quantification of C-14 carboxylic acids in the decontaminated leachate by LSC

The quantification of C-14 organic compounds was performed by using a typical Tri-Carb counter for the three fractions collected with a detection limit of 0.04 Bq/mL and an efficiency of detection of 72% in Ultima Gold LLT Liquid scintillation cocktail. Table 6 summarizes the activity obtained for 2 collected carboxylic acids expressed as CPM.

Table 6 Activities in the carboxylic acids collected fractions.

C-14 carboxylic acids	CPM	Bq/mL
Blank	3	
F4 - Oxalate	7 → 4	0.03
F5 - Butyrate	5 → 2	0.02

The activities measured in the carboxylic acids collected fractions were extremely low and under the detection limit of the device. These results confirm that C-14 carboxylic acid contents are lower than the detection limit of LSC. Consequently, the use of AMS is being

considered to allow the quantification of C-14 present as carboxylic acids in the collected fractions.

2.3 CEA contribution in WP3

CEA is in charge of three deliverables; D3.2 (issued in 2014), D3.7 (issued in May 2015) and D3.18 (due in January 2017). In 2016, CEA has launched leaching experiments under deaerated alkaline conditions on Zircaloy-based alloy hulls, supplied by AREVA and developed analyses for speciation of ¹⁴C and characterization of small organic molecules.

2.3.1 Materials Characterisations

As described in the previous annual report [NECIB, 2015], two different Zircaloy-based hulls supplied by AREVA have been studied: M5-type (UOX) and Zy-4-type (DUPLEX, MOX). After removal from PWR, these materials were treated in AREVA-La Hague. A second rinse treatment with nitric acid was also performed at Atalante facility in order to decrease the activity of the leaching samples.

Raman spectroscopy has been used to characterise the oxide layers formed at the metal surface. Several spectra were acquired at different locations on a M5 hull. Two examples are presented in Figure 4. The Raman bands correspond to ZrO₂ monoclinic phase [BARBERIS, 1997]. The spectra are very close to those obtained after zirconium alloy oxidation in PWR primary water conditions [VERLET, 2015]. Consequently, the acidic treatments performed at Areva La Hague and at Atalante have not changed the structure of the oxide layer that formed during irradiation in the PWR.

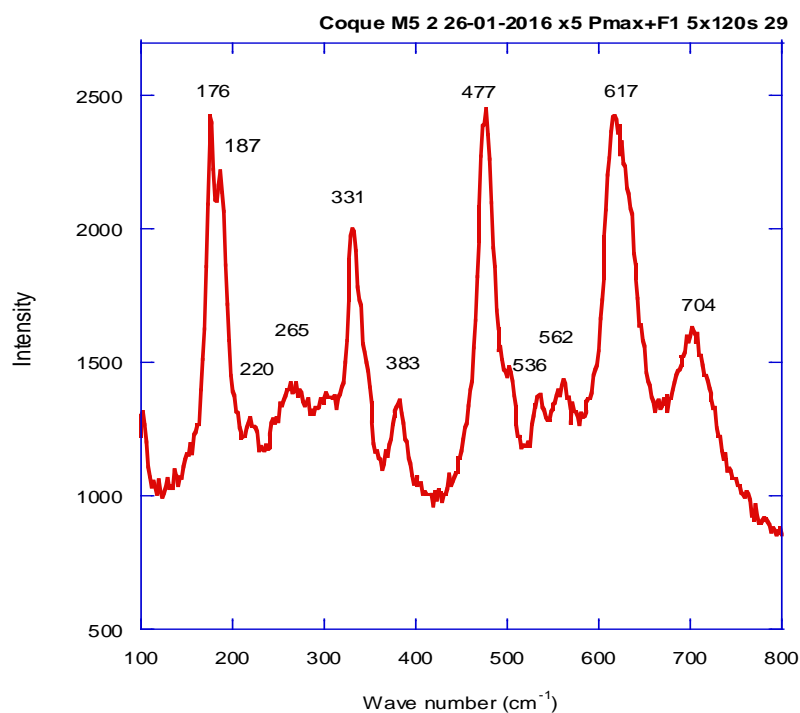
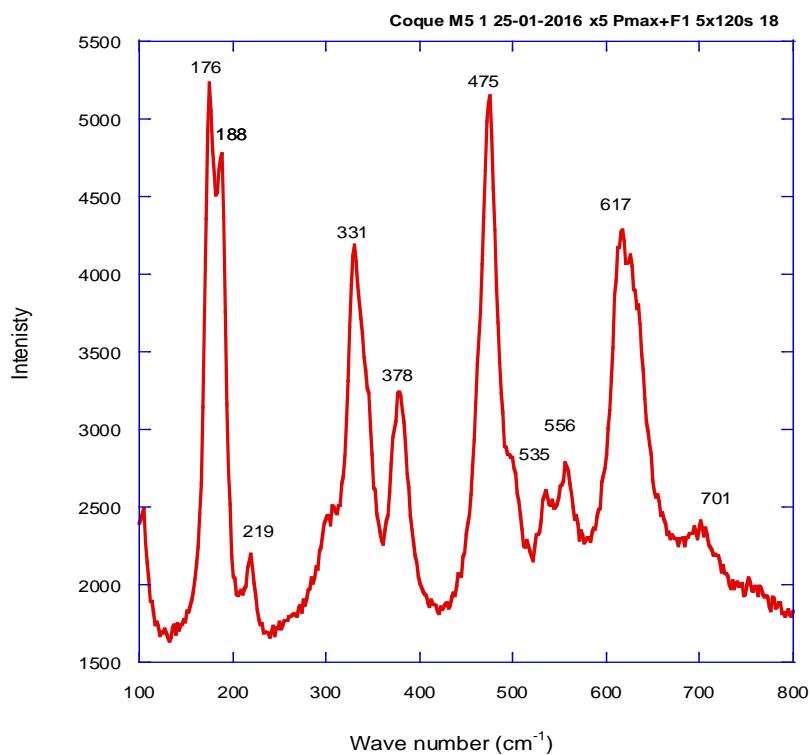


Figure 4 Raman spectra on irradiated M5TM hulls after acidic treatment during reprocessing

Likewise, Zy-4 hulls will be characterised in order to compare the oxide structure of the two different materials. In addition, optical observations on cross sections of the hull will be carried out in order to estimate the oxide thickness before the leaching experiments.

2.3.2 Leaching experiments

2.3.2.1 Preliminary test

Leaching experiments of the hulls have been performed in the DHA laboratory in Atalante facility (located in CEA Marcoule).

As described in CAST report D3.11 (NECIB, 2015), a preliminary test in aerated and alkaline solution of NaOH (235 ml) at pH 12 has been carried out on a M5-type hull during 14 days. The aims of this experiment were to check the feasibility of the radiochemical analysis in NaOH environment and to determine the activity of the solution according to the experimental parameters (volume, time, number of hulls...). From a safety point of view, this test validated the sampling to allow shipping to the laboratories in charge of C-14 analyses (CEA Saclay and Subatech Nantes).

After each sampling of solution, $\beta\gamma$ activities and α activity were measured by radiochemical counting. Figure 5 presents the results for a 30 ml sampling solution.

The maximum $\beta\gamma$ activities were about $840 \text{ Bq}\cdot\text{mL}^{-1}$ and 50.6 kBq. As shown in Figure 5 (red line) this value is below the $\beta\gamma$ activity limit acceptable at Subatech (1Mq). The maximum α activity was observed at the beginning of the experiment and is about $30 \text{ Bq}\cdot\text{mL}^{-1}$. For two hulls and a 30 mL sampling solution, the activity is equal to 1800 Bq which is below the α activity limit acceptable at Subatech (2000 Bq).

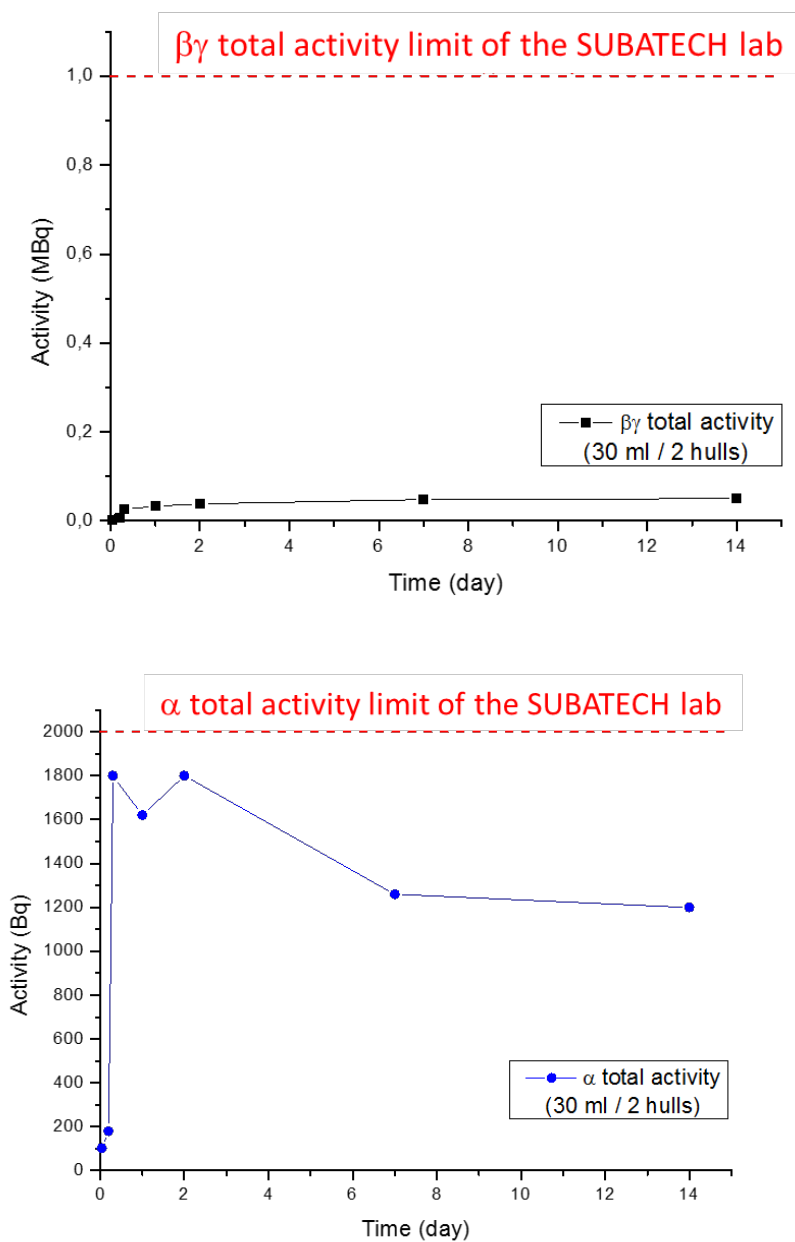


Figure 5 Evolution of total βγ activities (top) and α activity (bottom) during the preliminary test

2.3.2.2 Leaching test

The experimental set up for the leaching experiment was described in D3.11 [NECIB, 2015]. A volume of 235 mL of alkaline NaOH solution, pH 12, was introduced in the reactor with two M5-type hulls (total mass = 7.7g ; surface area ~ 40 cm²). After closing the leaching reactor, argon was sparged to de-aerate the medium. The final pressure was

maintained at 4.6 bar of argon. The temperature of the leaching test was about 30°C. The experiment started on 02/02/2016 under static condition (no renewal of solution) and two samplings of solution have been planned: one after 14 days and one after 5.5 months.

The first solution sampling (20 mL) and filtration (« millipore IC Millex-LH, PTFE hydrophile 0,45µm » filter) was carried out on 16/02/16. The measurement of the activity revealed an α activity of 60 Bq/mL and a βγ activity of 2300 Bq/mL. Consequently, between 5 and 6 mL of solution were sent to each laboratory in charge of C-14 analyses (CEA/DEN/DPC/SECR/LRMO, CEA/DEN/DPC/SEARS/LASE and Subatech).

Sampling after 5.5 month was performed early in August. Counting measurements revealed total activities below the limit of acceptability at the laboratories, therefore 30 mL of solution were sent to the three laboratories.

The leaching test of Zy-4-type hulls started early in September 2016.

2.3.3 Analytical strategy

Analyses have been carried out on a 14 day – leachate solution sampled from the leaching experiment performed with two M5-type hulls. In parallel, analyses have been carried out on a blank NaOH solution.

2.3.3.1 Carbon mass balance

Total organic and inorganic carbon

The analyses of organic (TOC) and inorganic (TIC) total carbon have been realized with a TC analyzer in a glove box. In 2015, the first calibration led to a detection limit around 1 mgC/L_{solution} in TOC and TIC (without sample dilution). The TIC and TOC results of blank and leachate samples are presented in Table 7.

Table 7 TIC/TOC results of blank and leachate samples.

	TOC (mgC/L)	TIC (mgC/L)
10⁻² M NaOH (Blank)	6 ± 1	7 ± 3
COQ M5B 14J A (Leachate)	11 ± 1	18 ± 2

Organic and inorganic carbon in the leachate of M5-type hulls after 14 days could be detected.

After subtraction of the amount of carbon detected in the blank sample, 5 mgC/L_{solution} were measured in the organic form in the leachate sample. It corresponds to 153 mgC/kg_{hull}.

If it is considered that all the TOC is in the form of oxalic acid form (carboxylic acid quoted in other leaching studies), it corresponds to 0.57 g_{acid}/kg_{hull}, namely 19mg_{acide}/L_{solution}. This content is above the detection and quantitation limits of ion chromatography (IC).

Total ¹⁴C determination

The determination of total ¹⁴C in the leachate sample has been realised on a tri-tube pyrolysis furnace manufactured by ERALY et associés. ¹⁴C trapped in the CarboSorb solution has been measured by Liquid Scintillation Counting (LSC) on a Tricarb 2910TR apparatus. The detection limit is around 0.3-0.5 Bq/mL of sample in the ceramic boat.

The total ¹⁴C results of blank and leachate samples are presented in Table 8.

Table 8 : Total ¹⁴C results of blank and leachate sample.

Sample	Total ¹⁴ C (Bq/g)
10 ⁻² M NaOH (Blank)	< LD LSC
COQ M5B 14J A (Leachate)	6.1 ± 0.5

6 Bq/g of total ¹⁴C in the leachate of M5-type hulls (14 days) could be detected. This corresponds to 3.7.10⁻² ng/g of total ¹⁴C in solution.

So, 186 Bq of ¹⁴C was released in leachate per gram of M5-type hull after 14 days. It corresponds to the release of 1.1 ng of total ¹⁴C per gram of M5-type hull. In term of the M5 surface area, 36 Bq of ¹⁴C was released in leachate per cm² of M5-type hull after 14 days. It corresponds to the release of 0.217 ng of total ¹⁴C per cm² of M5-type hull.

Organic and inorganic ¹⁴C partition

A method has been developed by the LASE laboratory. Tests were first conducted on a individual solution and on a mixture of two labelled organic and inorganic molecules (glucose ¹⁴C₆H₁₂O₆ and Na₂¹⁴CO₃) acidified with a solution of 25% H₃PO₄ under N₂

bubbling. The released CO₂ (inorganic C) was retained in a NaOH trap solution. The concentrations of the two carbon molecules were 70 Bq/g for glucose and carbonate at 110 Bq/g for carbonate in the mixture.

An aliquot of the NaOH trap solution was analysed by LSC to determine the inorganic ¹⁴C. The remaining solution in the reaction vessel was pyrolysed to measure the organic ¹⁴C. The organic and inorganic ¹⁴C partition results for the tests with the labelled molecules are presented in Table 9.

Table 9 Organic and inorganic ¹⁴C partition results of labelled molecules.

Sample	Inorganic ¹⁴ C	Organic ¹⁴ C
Na ₂ ¹⁴ CO ₃	85 %	0 %
¹⁴ C ₆ H ₁₂ O ₆	0 %	100 %
Na ₂ ¹⁴ CO ₃ + ¹⁴ C ₆ H ₁₂ O ₆	70 %	100 %

85 % of the inorganic ¹⁴C was trapped in the NaOH solution from the solution containing only ¹⁴C-carbonate and 70 % for the mixture. 100 % of organic ¹⁴C were detected by this method for the solution containing only ¹⁴C-glucose and for the mixture of the two labelled molecules.

So, inorganic ¹⁴C will be determined by the subtraction of measured organic ¹⁴C from the total measured ¹⁴C in the leachate sample.

This method was then applied to the M5-type leachate sample. Organic and inorganic ¹⁴C partition results of blank and leachate sample are presented in Table 10.

Table 10 Organic and inorganic ¹⁴C partition results of blank and leachate sample of M5-type hull.

Sample	Organic ¹⁴ C (Bq/g)	Inorganic ¹⁴ C (Bq/g)
10 ⁻² M NaOH (Blank)	< LD LSC: 0.5 Bq/ml	< LD LSC: 0.5 Bq/ml
COQ M5B 14J A (Leachate)	2.8 ± 0.4 (meas)	3.3 ± 0.4 (calc)

2.8 Bq/g of organic ^{14}C in the leachate of M5-type hulls (14 days) was detected. It corresponds to $1.7 \cdot 10^{-2}$ ng/g of organic ^{14}C . Inorganic ^{14}C in trap solution was below the detection limit of LSC, and the value indicated in Table 10 was calculated from the measured total ^{14}C given in Table 8 and the organic ^{14}C . The trap solution will also be measured by accelerator mass spectrometry (AMS).

In the leachate of M5-type hulls, 6.1 Bq/g of total ^{14}C were detected and the partition of ^{14}C was: 46 % organic and 54 % inorganic.

The organic C-14 is not overestimated as when a carbonate solution is used alone, all the C-14 is detected in the trapped solution and no inorganic C-14 is kept in the vessel reaction.

To explain the results for the carbonate solution, a 2M NaOH solution can be used. To have a better recovery, a 5 M NaOH solution was used. However, with a 5M NaOH solution, it is not possible to do the LSC directly. Dilution is performed on the trap solution. With these tests it was shown that the acidification by H_3PO_4 has no effect on organic C-14 and the inorganic C-14 is released as CO_2 with no remaining in the vessel.

2.3.4 Speciation

IC was used to identify and quantify carboxylic acids in the leachate sample in a glove box. One method was already developed for the detection of 10 carboxylic acids in high NaOH concentrations, as shown in Figure 6. The detection limit was estimated at $1 \text{ mg}_{\text{acide}}/\text{L}_{\text{solution}}$ NaOH solution. A calibration curve was also realised between 1 and $10 \text{ mg}_{\text{acide}}/\text{L}_{\text{solution}}$.

The blank and leachate sample were analysed with the same IC. The results are presented in Figure 6.

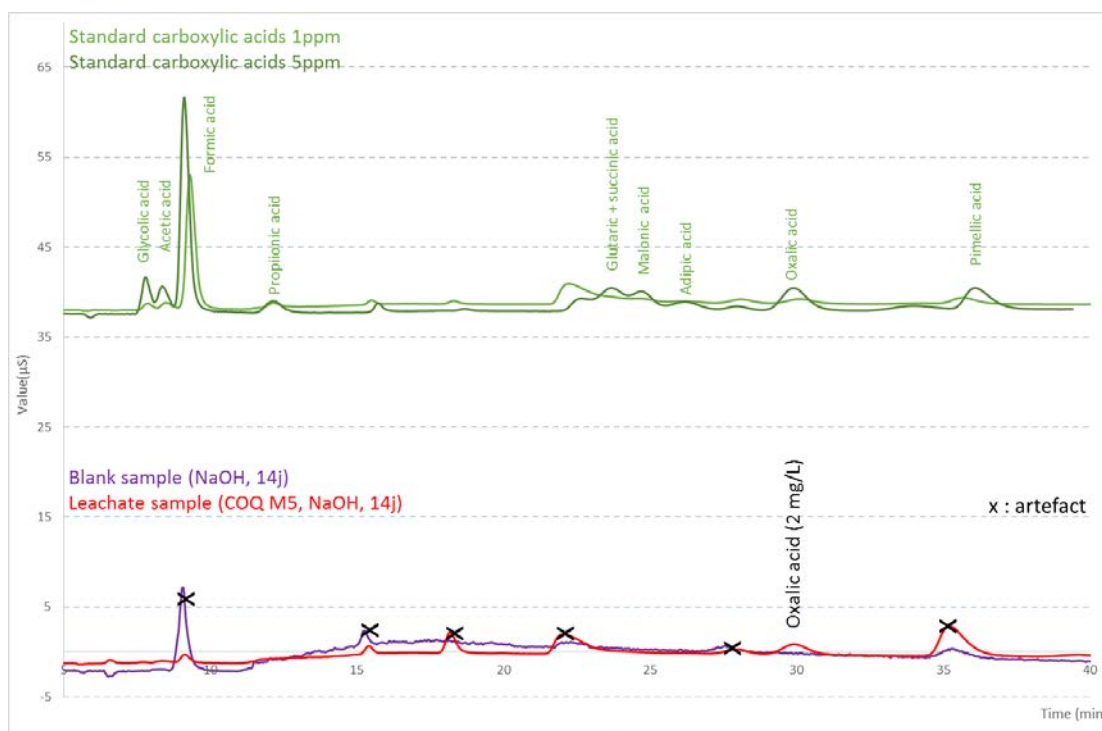


Figure 6 Results obtained by IC (blank sample in purple, leachate sample in red and standards for carboxylic acids in green)

Many peaks could be detected for the leachate sample, despite the very low signal. Black crosses highlight the peaks also present in the blank sample. At a retention time of 30 minutes, one peak was observed in the leachate sample only. It corresponds to oxalic acid. From the calibration curve a concentration of $2 \text{ mg}_{\text{acide}}/\text{L}_{\text{solution}}$ can be estimated, which represents $0.5 \text{ mgC}/\text{L}_{\text{solution}}$ namely 10.6 % of the TOC.

2.3.5 Conclusions

Table 11 summarises the analytical strategy at CEA as well as the progress in 2016.

Table 11 Analytical techniques and associated goals obtained since the 2nd annual report (D3.11).

	Technique	Advance
CARBON MASS BALANCE	TIC/TOC	Detection limit around 1 mgC/L _{solution}
	Total ¹⁴ C	Detection limit by LSC around 0.5 Bq/mL and by AMS around 0.5 mBq/mL Recovery of ¹⁴ C by pyrolysis above 90% for liquid samples
	TIC/TOC ¹⁴ C	100 % of organic ¹⁴ C is detected by the method – inorganic ¹⁴ C is calculated
SAMPLE PREPARATION	Filtration	No improvement of desalination with ion exchange resin: 30-40 % of carbon is always lost
ORGANIC SPECIATION	FTIR	Detection limit too high
	IC	Analysis of 10 carboxylic acids without ¹⁴ C detection Detection limit around 1mg _{acide} /L _{solution}
	GC-MS	According to sample activities for experiments in the glove box
	ESI-MS	ESI-MS could be done but without filtration

Table 12 summarises the results obtained for the leachate sample of M5-type hull after 14 days.

Table 12 Results of leachate sample of M5-type hulls after 14 days.

Sample	Total ¹⁴ C (pg/g)	Organic / inorganic partition	
COQ M5B 14J A	37 ± 3	46 %	54 %
	Total Carbone (mgC/L)	TOC (mgC/L)	TIC (mgC/L)
	16 ± 4	5 ± 1	11 ± 3

Figure 7 presents the carbon mass balance (CMB) of the leachate sample.

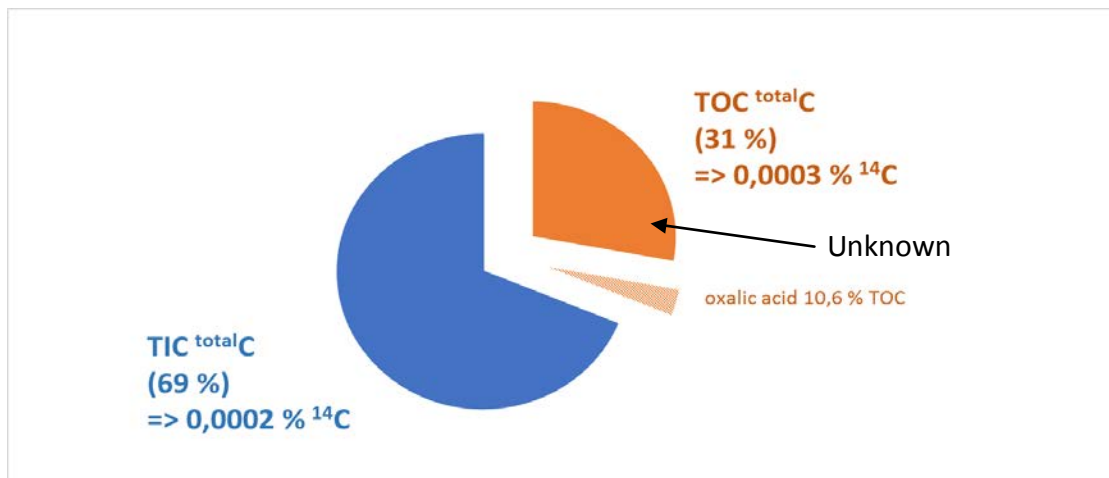


Figure 7 Carbon mass balance of the leachate sample

TIC corresponds to 69 % of CMB and the ¹⁴C represents 0.0002 % of TIC. TOC corresponds to 31 % and ¹⁴C represents 0.0003 %. Oxalic acid represents 10.6 % of TOC. Around 90 % of TOC has not been identified and quantified yet. To complete the CMB, GC-MS analyses have been carried out.

2.4 ITU / JRC contribution in WP3

Within WP3, ITU/JRC is in charge of two deliverables; D3.6 (issued in 2015) and D3.14 (due in January 2017).

2.4.1 Non irradiated materials

The irradiated cladding test material from the Gösgen reactor is a duplex cladding of Zircaloy-4 with a thin external Zr-2.5Nb cladding. Details of the fuel were given in a previous report (D3.6). As it is important to know the C, N & O contents of the cladding, non-irradiated samples of a commercial Zircaloy-4 cladding was analysed at ITU for these values as well as verifying the major metallic elements.

The main analytical technique was ICP-MS for the metallic elements, while the inorganic elements (C, N, O) were measured by a metallurgical hot extraction technique to more accurately determine the elements that are responsible for C-14 production in the cladding.

The values are shown in Table 13 and Table 14. It shows 1.2Sn -0.2Fe-0.1 Cr as expected from the specifications. It is noted that the C determination was imprecise in the first

determination (only an upper limit could be given) due to a poor functioning of the device. However the impurities, N and O have been determined with more accuracy. Table 14 shows O ~1200ppm C <500ppm, N ~ 45ppm.

Table 13 Chemical composition from ICPMS measurements (these are given as an uncertainty range of 2k= 2x standard deviation and so represents 95% confidence level within this range)

Sample ID	Measurand	Concentration ± Uncertainty (µg/g) [k=2]	Measurement date	Reference date
Zry4-a	Hf	61.5 ± 7.4	15-10-2015	N.A.
	B	< 140		
	P	< 32		
	Sn	12396 ± 1488		
	Ni	38.0 ± 4.6		
	Fe	2240 ± 269		
	Cr	1174 ± 141		

Remarks: If no result is given, the value is below the quantification limit. The value stated as Uncertainty is then the actual quantification limit.

Table 14 Chemical composition from ELemental ANALysis (ELANA) measurements (hot extraction)

Sample ID	Measurand	Concentration ± Uncertainty (wt%) [k=2]	Measurement date	Reference date
Zry4-b	O	0.117 ± 0.019	11-11-2015	N.A.
	C	< 0.05		
	N	0.0044 ± 0.0102		

Observation: Due to some technical issues with the instrument, it was not possible to provide quantitative results for the carbon content.

Nitrogen and carbon were remeasured and Table 15 indicates that the actual carbon concentration is in fact far lower than the upper limit from the first measurements and is approximately 90 ppm.

Table 15 Retesting of non-irradiated small ring samples of Zircaloy-4 (firm Bruker AXS GmbH, Karlsruhe).

Cladding	Carbon Content (ppm)		Nitrogen content (ppm)	
	1 st test	Retesting	1 st test	Retesting
Zircaloy -4	<500 ppm	91 +/- 3 ppm (3 samples x 0.4g)	44 +/-10 ppm (4 samples x 0.5g)	31 +/-5 ppm (5x 0.1g samples)

2.4.2 Modelling

The above values could be used (including now the lowered C content of 90 ppm for Zircaloy-4 and the slightly revised N content: 31ppm instead of 44ppm) for modelling the expected inventory for the cladding materials. KIT-INR has already performed some initial calculations using this data and for that of INE's irradiated cladding (D3.8) [HERM, 2015-a]. This preliminary data suggests an approximate value of 1.3×10^4 Bq /g Zircaloy-4 cladding (based on estimated 270 ppm C). There are no measurements at ITU to compare with these modelled values. Modelled estimates of INE's samples (with a more accurate C value) appear to correspond well to their measurements. It is difficult to say what is the relative impact the slight change in N would have on the overall C-14 value, as both C and N values were lowered and would both reduce the modelled C-14 estimate.

2.4.3 Leaching test

2.4.3.1 Samples

Samples have been cut as 3mm long rings (1-0.5g). The Zircaloy-4 cladding has been defueled. 4 Zircaloy samples were cut at fuel height from the upper end of the rod. The fuel has been pressed out with a die, followed by HNO₃ immersion for removal of the remaining fuel (2x 15 mins in 8M HNO₃), rinsed followed by a final ultrasonic clean in distilled water for 15mins then finally dried in air. This may affect the external oxide film. However the inner surface appears to be clean and to have a bluish hue to the inner metallic surface (see Figure 8).

The samples have been weighed, then before testing, the samples will have dose rate measurements and then gamma spectroscopy. Measurements on samples or the solutions

after leaching will be used to detect any corrosion/estimate corrosion rates. For comparison non-irradiated samples will be degreased in alcohol, rinsed in water and then air-dried and weighed before testing.



Figure 8 (left): Dark film on inner surface seen after first acid clean. Little difference is seen after second acid clean; (right): pieces of fuel after defueling.

2.4.3.2 Autoclaves for leaching tests

ITU will use an existing stainless steel autoclave that has been adapted by replacing the PTFE lining by a PEEK lining (Figure 9). A heating plate & jacket is available (one inside the cell and another in reserve) and will be used for the higher temperature test at 80°C by using the thermocouple in the heating block for approximate but more robust temperature control. The other tests at 30°C will be effectively at ambient hot cell temperatures. Tests will be of 3 months length with a single sampling (gas & liquid) at the end of the test. The pressure will be 1-2 bars. A gas mouse with special connections was fabricated for ease of connection and detachment and the autoclave was designed with matching connections. However during a visit to INE (July 16) to examine the method in detail, it was noted that the connection system was not sufficiently airtight to take a good sample from the autoclave without contamination transfer to the glove box. Therefore, new connectors for the gas mouse were ordered; new connectors were also needed for the autoclave and glove box.

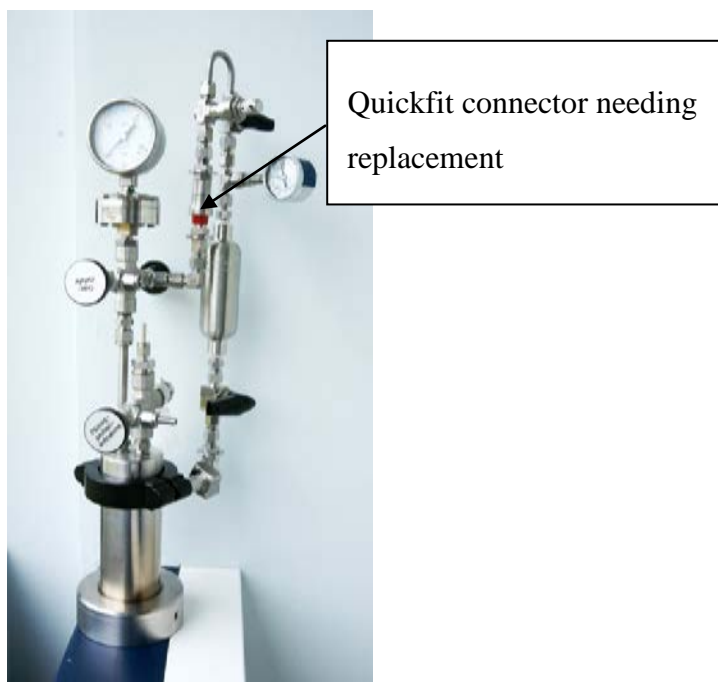


Figure 9 Autoclave with gas mouse attached. The connection requires improvement in order to allow optimum sampling and avoid transfer of contamination to the C-14 analytical glove box.

In order to try to recover time, new autoclaves have been purchased to perform the non-irradiated testing capable of 10 bar up to 100°C; they have a borosilicate glass base and a PTFE cover with a sampling port. They need an injection/extraction system adding for sampling and transfer to the glove box line.

In addition, the purchase of further 150ml (200bar) stainless steel autoclave with PEEK lining is underway in order to increase the capacity for testing for the irradiated cladding samples.

2.4.4 C-14 analyses

2.4.4.1 Glove box

The analytical glove box is under preparation for C-14 analyses. The following tasks have been performed:

- The furnace & round-bottomed flask heating have been tested; the balance was tested, stand for wash bottles set up, bottles mounted and gas lines connected (clasps to be ordered). Flowmeters and pumps installed and tested,

- Water cooling for the condenser of the flask (& pump) have been installed along with glove box filters on top of the glove box,
- Protective metallic grids have been installed to prevent glove contact from hot surfaces on furnaces and tested.

Testing still needs to be on the gas line tightness with better clamps (already ordered). The glove box will be set up in wing B on a gallery area behind the hot cells together with its atmosphere purification system. The gas mouse connection system on the glove box needs to be added as well as fabrication of the gas mouse itself (see Figure 10 and Figure 11).



Figure 10 Photograph showing the additional work on the glove box roof: glove box filter system and glove box lighting placed on top.



Figure 11 Horizontal view with the heating element and furnace with the additional shielding for protection against hot areas during operation of the furnaces.

2.4.4.2 Total carbon content measurements

A HF ICARUS G4 device has been purchased from Bruker, Karlsruhe. It can measure total inorganic carbon content of metallic samples. It has been designed specially with the transformer & rectifier separated from the induction furnace (where the sample is oxidised and CO₂ produced) and placed outside. In addition, much of the analytical components will remain outside the hot cell. After construction and initial testing at Bruker, delivery and successful commissioning took place at JRC-ITU-Karlsruhe in July 2016. The device is now awaiting for final cleaning of the lead hot cell. The hot cell can then be opened and the device installed and connected up. A small glove box will be added (in front of the hot cell

next to the analysis unit) to include a filter on the exhaust gas line, collect all the CO₂ in the line for transfer to the C-14 analytical GB for analysis. It is expected that the installation in the hot cell of the device will take place by the end of the year with active operation in 2017.

2.4.5 Overall schedule

The first irradiated test is planned to start by October 2016 on 3 Zry samples. Non-irradiated samples will be done in parallel. This assumes post-test analysis (gamma-spectroscopy) as well as metallography & SEM-EDS of selected samples.

The next aspect is the operation of the glove box. If this is ready by late 2016 with testing by using C-14 calibration sources for verification, then it could be in operation from early 2017 to do all C-14 analyses of the gases and leach solutions.

Finally the installation of the Bruker device in the hot cell is due to be carried out by the end of the year; final adaptations to the glove box for the C-14 collection in the molecular sieve could be completed by early 2017. This could then be used for doing the key samples by April- June 2017.

2.5 KIT contribution in WP3

Within WP3, KIT is in charge of three deliverables; D3.3 (issued in 2014), D3.8 (issued in 2015) and D3.15 (due in January 2017).

2.5.1 Introduction

After the commissioning of a specifically manufactured glove box in May 2014 and the successful development of the C-14 separation, quantification and speciation methods in the beginning of 2015, KIT started acidic dissolution experiments involving irradiated Zircaloy-4 cladding specimens sampled from the plenum of a fuel rod segment irradiated in the Swiss Gösigen PWR. Following further improvements of the separation and analysis methods, C-14 was successfully separated in aqueous and gaseous samples in the second half of 2015. In parallel, Monte Carlo N-particle (MCNP-X) activation calculations were performed to

determine the radionuclide inventory in the irradiated material taking into account the specific irradiation history of the plenum cladding in the Gösgen PWR.

In 2016, focus was given on the evaluation of the data obtained from the separation and analysis of C-14. The improvement of the C-14 extraction/separation technique as well as the results obtained for the C-14 inventory present in irradiated Zircaloy cladding and the chemical form of C-14 after release from irradiated material are summarized in the following sections.

2.5.2 Improvement of the separation technique

Tritium as gaseous $^1\text{H}-^3\text{H}$ (HT) is quantitatively released during digestion of irradiated Zircaloy [NEEB, 1997]. In contrast to $^1\text{H}-^3\text{H}-\text{O}$ (HTO), large amounts of gaseous HT passes through the first four washing bottles of the extraction system [HERM, 2015-a] unaffectedly. A catalytic furnace, installed after the first four washing bottles, oxidizes the HT to HTO. This HTO is then absorbed in alkaline washing bottles after the furnace and disturbs significantly the quantification of C-14 present in these traps. In order to remove the HTO, two additional washing bottles containing dilute sulphuric acid were added to the extraction system between the furnace and the alkaline C-14 traps.

In Figure 12 the LSC spectrum obtained from the first alkaline washing bottle after the furnace is shown. Since no additional tritium trap after the furnace was used, the vast majority of HT was oxidized to HTO in the furnace and trapped together with C-14 (as $^{14}\text{CO}_2$) in the alkaline bottle. The installation of one additional tritium trap after the furnace shows already a significant improvement. However, a tritium peak is still visible in the LSC spectrum of the C-14 trap following the tritium trap (see Figure 12b). Therefore, a second tritium trap after the furnace was installed. Figure 12c shows the LSC spectrum received for the alkaline C-14 trap after the furnace and the two tritium traps. Only a single peak attributed to C-14 was obtained and as a consequence, C-14 was successfully separated from tritium and all other radionuclides present in the digestion liquor or gas phase.

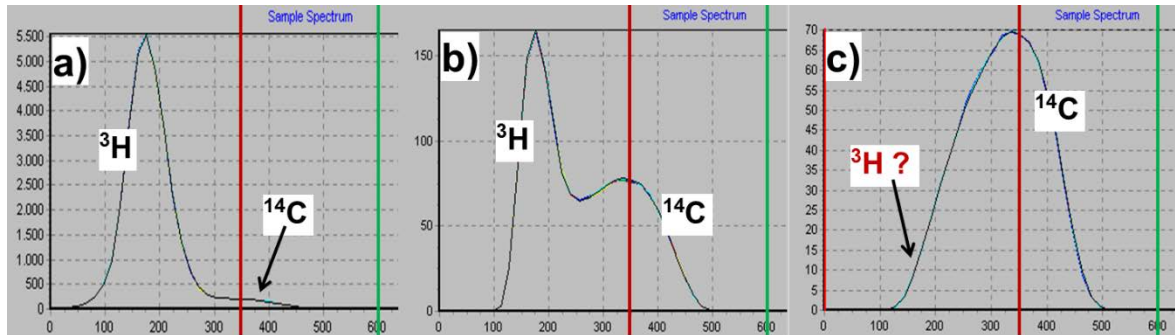


Figure 12: LSC spectra obtained from first alkaline washing bottle after the furnace of the C-14 extraction system. a) LSC spectrum obtained for the alkaline C-14 trap without additional tritium trap after the furnace; b) LSC spectrum of the C-14 trap with one additional tritium trap after the furnace; c) LSC spectrum obtained for the C-14 trap with two additional tritium traps installed after the furnace.

2.5.3 Inventory and chemical form of C-14

Results of the experimental inventory analysis of each of six Zircaloy-4 cladding specimens are shown in Table 16. A good reproducibility of the determined C-14, Fe-55, Sb-125, and Cs-137 activities within the analytical uncertainty can be seen. The results demonstrate the reliability of the C-14 extraction and analysis method for both dissolution approaches (glass reactor/autoclave) used in this work [HERM, 2015-b].

Table 16 Results obtained from LSC and γ -measurements from six Zircaloy-4 cladding specimens.

sample no.	total C-14 [Bq/g Zry-4]	Fe-55 [Bq/g Zry-4]	Cs-137 [Bq/g Zry-4]	Sb-125 [Bq/g Zry-4]
#1	$3.9 (\pm 0.4) \times 10^4$	$1.3 (\pm 0.1) \times 10^5$	$3.7 (\pm 0.2) \times 10^6$	$2.6 (\pm 0.1) \times 10^5$
#2	$4.2 (\pm 0.4) \times 10^4$	ND	$3.2 (\pm 0.2) \times 10^6$	$2.4 (\pm 0.1) \times 10^5$
#3	$3.4 (\pm 0.3) \times 10^4$	ND	$3.8 (\pm 0.2) \times 10^6$	$2.5 (\pm 0.1) \times 10^5$
#4	$3.2 (\pm 0.3) \times 10^4$	ND	$3.8 (\pm 0.2) \times 10^6$	$2.3 (\pm 0.1) \times 10^5$
#5	ND	$1.7 (\pm 0.2) \times 10^5$	$3.3 (\pm 0.2) \times 10^6$	$2.5 (\pm 0.1) \times 10^5$
#6	$3.8 (\pm 0.4) \times 10^4$	ND	$2.6 (\pm 0.1) \times 10^6$	$2.2 (\pm 0.1) \times 10^5$

ND: not determined

Furthermore, mean values of the experimentally determined radionuclide inventories are shown in Table 17 and compared to the MCNP-X calculations performed in this study. Within the analytical uncertainty, the experimentally obtained results in this study for the inventories of C-14, Fe-55 and Sb-125 are in very good agreement with calculation. The

experimental C-14 inventory is consistent with the calculated value. In contrast, the experimental C-14 inventory in an irradiated stainless steel, recently assessed by [SCHUMANN, 2014], exceeds the calculated value by a factor of four. Additionally, the C-14 inventory determined in this study is in good agreement with experimental data of a similar PWR fuel rod hull specimen provided by [YAMAGUCHI, 1999].

However, the experimental Cs-137 inventory exceeds the calculated value by a factor of 117. The excess of Cs-137 is attributed to the precipitation of Cs-137 on the inner Zircaloy cladding surface, possibly released during reactor operation from subjacent UO₂ pellets. The additional Cs-137 inventory is not taken into account in the MCNP-X calculation, since the neutronic simulation does not include the migration of volatile elements.

Table 17 Mean values of the experimentally determined inventories of C-14, Fe-55, Cs-137 and Sb-125 in comparison with results from the activation calculations performed in the present study and experimentally measured C-14 contents in a spent PWR Zircaloy-4 specimen with a similar average burn-up [YAMAGUCHI, 1999].

	C-14 [Bq/g Zry-4]	Fe-55 [Bq/g Zry-4]	Cs-137 [Bq/g Zry-4]	Sb-125 [Bq/g Zry-4]
measured contents in Zry-4 of segment SBS1108–N0204 (50.4 GWd/t_{HM}) [p.w.]				
calculated contents in Zry-4 of segment SBS1108–N0204 (50.4 GWd/t_{HM}) [p.w.]				
measured contents in Zry-4 of spent PWR fuel rod hull specimen (47.9 GWd/t_{HM}) [Yamaguchi, 1999]				
	$3.7(\pm 0.4) \times 10^4$	$1.5(\pm 0.1) \times 10^5$	$3.4(\pm 0.2) \times 10^6$	$2.4(\pm 0.1) \times 10^5$
	$3.2(\pm 0.3) \times 10^4$	$1.3(\pm 0.1) \times 10^5$	$2.9(\pm 0.1) \times 10^4$	$2.6(\pm 0.1) \times 10^5$
	3.2×10^4			

The partitioning between the total inorganic and organic C-14 fractions for each of the analysed specimens is shown in Table 18. The extraction systems has two sets of alkaline washing bottles. The first set is for trapping ¹⁴CO₂ released during acid digestion in a flask or autoclave (inorganic fraction) while e.g. ¹⁴CH₄ passes through these alkaline bottles unaffectedly and is trapped in the second set of alkaline washing bottles (organic fraction) after oxidation in a furnace after the first set of C-14 traps. The analytical set-up and extraction procedure is described in detail elsewhere [HERM et al., 2015 and HERM 2015-b].

Again, a good reproducibility of the results, within the analytical uncertainty, confirms the reliability of the method. Also, virtually no differences between two dissolution approaches (glass reactor/autoclave) used in this study are seen. In all experiments, the vast majority of C-14 is found in the organic fraction, whereas almost no inorganic C-14 is found.

Table 18 Partitioning of C-14 between total inorganic C-14 (TIC-14) and total organic C-14 (TOC-14) fractions for each analysed specimen.

sample no.	TIC-14 [Bq/g Zry-4]	TOC-14 [Bq/g Zry-4]
#1	$9.5 (\pm 0.1) \times 10^1$	$3.9 (\pm 0.4) \times 10^4$
#2	$11.9 (\pm 0.1) \times 10^1$	$4.2 (\pm 0.4) \times 10^4$
#3	$11.8 (\pm 0.1) \times 10^1$	$3.4 (\pm 0.3) \times 10^4$
#4	$6.2 (\pm 0.1) \times 10^1$	$3.2 (\pm 0.3) \times 10^4$
#5	ND	ND
#6	$10.4 (\pm 0.1) \times 10^1$	$3.8 (\pm 0.4) \times 10^4$

ND: not determined

Autoclave experiments provided insight into the distribution of the inorganic/organic C-14 compounds released during acid digestion into the aqueous and gaseous phases. The partitioning of C-14 bearing compounds in inorganic/organic fractions and their distribution into the aqueous and/or gaseous phase is shown in Table 19. About $(88 \pm 10)\%$ of the C-14 inventory present in irradiated Zircaloy-4 is released as gaseous organic C-14 bearing compounds during dissolution into the gas phase. On the contrary, about $(11 \pm 10)\%$ remains as dissolved organic C-14 bearing compounds in the acidic digestion liquor. Almost no inorganic C-14 bearing compounds ($< 1\%$) are found in all experiments (glass reactor/autoclave) neither in the gaseous nor in the aqueous phase.

Table 19 Distribution of inorganic/organic C-14 bearing compounds in the aqueous and gaseous phase obtained from dissolution experiments performed in an autoclave.

	inorganic C-14		organic C-14	
	mean activity [Bq/g Zry-4]	fraction in %	mean activity [Bq/g Zry-4]	fraction in %
aqueous phase	$1.0 (\pm 0.1) \times 10^1$	< 1	$4.0 (\pm 0.4) \times 10^3$	11.4 ± 10
gaseous phase	$7.2 (\pm 0.7) \times 10^1$	< 1	$3.1 (\pm 0.3) \times 10^4$	88.4 ± 10

2.5.4 Summary and conclusions regarding the inventory and chemical form of C-14 in Zircaloy-4

Using the C-14 separation and analysis techniques developed in this work for gaseous and aqueous samples derived from acid digestion of irradiated Zircaloy-4 specimens, it was possible to quantify the C-14 content in these samples. Furthermore, the partitioning of C-14 between inorganic and organic C-14 bearing compounds and their distribution between solution and gas phase was investigated. In addition to C-14, the contents of Fe-55, Sb-125 and Cs-137 in irradiated Zircaloy-4 were analysed and also compared to MCNP-X calculations.

The vast majority of C-14 is released from irradiated Zircaloy-4 as hydrocarbons into the gas phase (about 88%) and aqueous phase (> 11%). Almost no (< 1%) inorganic C-14 bearing compounds (e.g. carbonates, bicarbonates) were found in all experiments (glass reactor as well as autoclave) conducted with irradiated Zircaloy-4. Also remarkable is the similar ratio between inorganic and organic C-14 bearing compounds in the aqueous phase (1:390) and gas phase (1:430).

The comparison of experimental and theoretically predicted contents of various radionuclides (C-14, Fe-55, and Sb-125) and their good agreement further proves the reliability of the obtained data. The experimentally determined activities of the activation products in the irradiated Zircaloy-4 agrees within a factor < 2 with the MCNP-X calculation, except for the fission product Cs-137. The difference is considered as relatively small taking into account the limited availability of data for the calculations.

Despite extensive testing of the separation technique by dissolving non-irradiated Zircaloy, the interference of gaseous HT, quantitatively released from irradiated Zircaloy-4 during digestion, and its oxidation to HTO was not taken into account and modifications of the separation technique were necessary.

Although the digestion experiments were performed under acidic conditions, clearly outside of repository-relevant conditions, little impact on the chemical form of C-14 released from irradiated Zircaloy under repository relevant conditions is expected. The vast majority of C-14 is found as dissolved/gaseous hydrocarbons and almost no dependency on the pH is expected for the speciation of organic compounds. In addition, strongly reducing conditions

potentially developing in a deep underground repository for nuclear waste favours the formation of reduced/organic C-14 compounds. The similar outcome of experiments performed in this study under acidic conditions, room temperature and N₂ or Ar atmosphere and [BLEIER, 1988] using HF, NaCl or NaCl–NaF, 200°C and air atmosphere further support this assumption.

The developed C-14 extraction and analysis methods described in this study for irradiated Zircaloy-4 are not only very reliable but can also be applied in future investigations with other structural parts such as stainless steel or SNF itself of a fuel rod.

Leaching experiments under neutral/alkaline conditions are foreseen. However, these experiments will be conducted likely outside of the CAST project since the final reports in WP3 are already due in January 2017. KIT is currently dealing with irradiated steel (WP2) which is, due to the high dose rate (> 100 mSv/h per specimen), a much more demanding/time-consuming task.

2.6 *RATEN ICN contribution in WP3*

RATEN ICN is in charge of D3.16 (due in January 2017).

2.6.1 *Leaching tests on irradiated Zy-4 samples*

The leaching tests started in April 2016 for the irradiated samples and in June 2016 for un-irradiated samples.

6 samples of irradiated Zy-4 were available for the leaching tests. These samples were obtained from a CANDU spent fuel bundle that was irradiated for 1 year in the Cernavoda NPP Unit 2 and kept for cooling 4 more years in the Spent Fuel cooling bay. After the cooling period, the fuel bundle was transported to RATEN ICN for different investigations and in the last 2 years it was stored in the ICN hot cells.

Preliminary SEM investigations on the CANDU spent fuel were performed. The thickness of the zirconium oxide layer measured along the fuel tube was between 3 µm and 3.5 µm. Based on the communication of the fuel producers (FCN Pitesti), the nitrogen content in Zy-4 is 30 ppm.

To be able to correlate the C-14 content with the Co-60 content, gamma measurements were carried out on the samples before starting the leaching tests. Gamma scanning will also be performed to measure the Co-60 content in the leachate solution.

Due to the high content of Cs-137 in the irradiated Zy-4 samples, gamma measurements were performed on small rings cut from the irradiated Zy-4 to be used in the long term leaching tests. An ORTEC Gamma spectrometer with HPGe detector was used for these measurements and results are reported as Bq per gram of irradiated Zy-4 as presented in Table 20. Figure 13 presents a spectrum showing the main gamma emitters.

Table 20 Main gamma emitters identified in the irradiated Zy-4

Radionuclide	Co-60	Cs-137	Cs-134	Sb-125
Activity [Bq/g]	1.601 E+05	5.4895 E+06	5.676 E+05	6.193 E+06

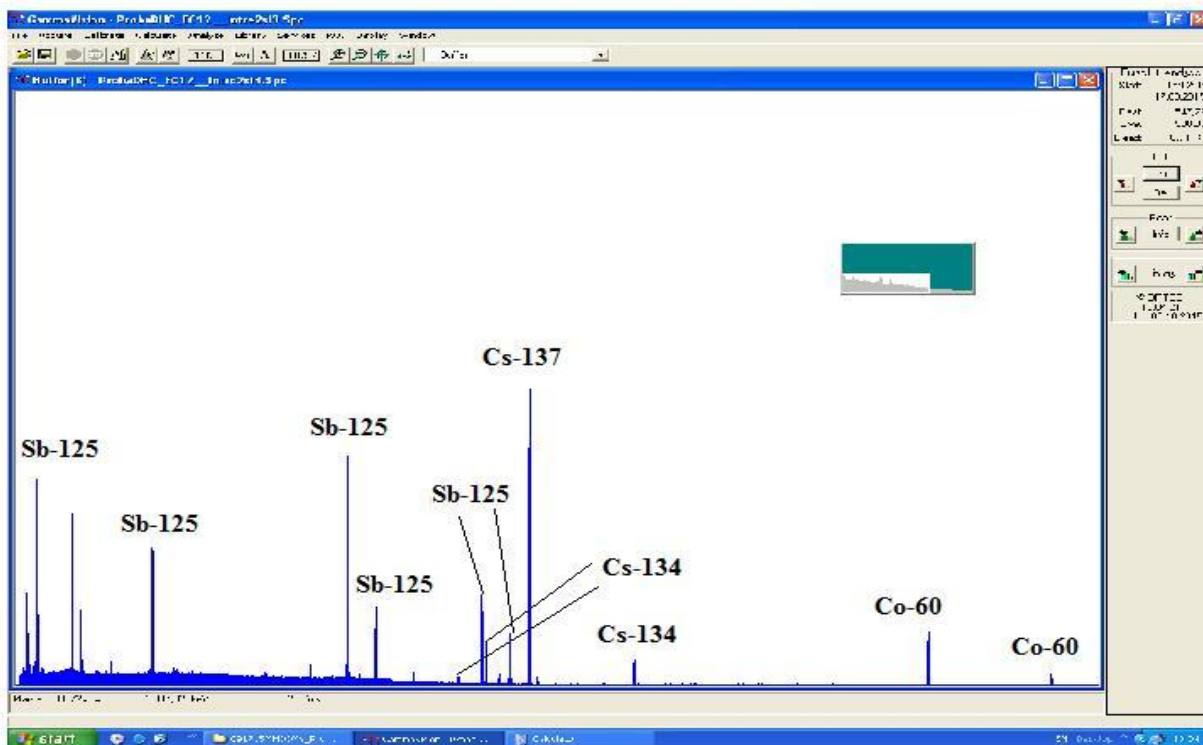


Figure 13 Spectrum with the main gamma emitters

Each of the six samples, available for the experimental programme proposed under CAST, was cut in two pieces: a small one for C-14 measurement and a larger one to be immersed in deaerated NaOH solution (pH ~ 12).

Static leaching tests have been run under N₂ atmosphere. Six glass tubes (2 tubes for three different leaching time: 6 months, 8 months and 12 months) were adapted to allow N₂ purging for 24 hours in order to ensure anoxic conditions (Figure 14). Due to the high radiation dose, the glass tubes were placed inside of a lead castle. The total C-14 content and its inorganic / organic partition in the leachate solution will be carried out by the end of the year 2016.

After 6 months (by October 2016), the first two tubes will be open to sample the leachates in order to measure both total C-14 and its inorganic / organic partition. Before opening the tubes, N₂ will be purged and the gas will be washed in gas washing bottles in order to absorb the inorganic C-14 that could be released as gas during these six months. The LSC technique will be used to quantify C-14.

After the removal of the leachate solution, two irradiated Zy-4 samples will be used for electrochemical tests. The experimental setup consists of an AUTOLAB 302 electrical potentiostat/galvanostat connected to a glass cell equipped with a Pt counter electrode, an Ag/AgCl reference electrode and the Zy-4 working electrode.



Figure 14 View of the six glass bottles used in the leaching tests

C-14 released in the liquid phase will be analysed by LSC using a TRICARB 3110 TR counter allowing C-14 measurements in ultra-low levels with typical count rate in the range of 1-20 CPM above the background. To measure the inorganic and organic C-14, a method based on a combination of acid stripping and wet oxidation will be used.

2.6.2 Modelling the C-14 accumulation in CANDU Zy-4 tube during fuel irradiation

The accumulation of the C-14 in the CANDU Zy-4 tube was evaluated by using the ORIGEN code. The simulation gives a C-14 inventory in the Zy-4 cladding around $1.776 \cdot 10^4$ Bq/g (0.481 μ Ci/g) of Zy-4.

Modeling of the C-14 accumulation was achieved by using ORIGEN-S and SCALE 4.4 codes for an irradiation time of CANDU fuel of 890 days and a thermal flux of $4.5E13$ nv.

CANDU fuel assembly contains 37 elements comprising of sintered UO₂ pellets (30 pellets of natural uranium) in Zy-4 tubes. The 37 elements are circularly arranged on three rings of 18, 12 and 6 elements respectively, around a central element. A particularity of CANDU fuel is the colloidal graphite (CANLUB) deposited on the inside surface of the Zy-4 tubes (the average thickness of the graphite layer is 5 μ m with a minimum of 3 μ m). Therefore, the C-14 accumulated in the irradiated Zy-4 is a combination of the C-14 formed or attached on the oxide layer, the C-14 formed in the Zy-4 metal but also small amount of C-14 formed in the graphite layer.

The characteristics of CANDU core and fuel bundle are presented in Table 21, while the composition of the Zy-4 in Table 22.

Table 21 CANDU core and fuel bundle characteristics

Natural uranium weight	18.7 kg
Fuel bundle weight	23.5 kg
No of fuel bundles in a fuel channel	12.0
Number of fuel channels	380
Number of fuel bundles in the core	4560
Average burn up	7 MWd/kgU
Weight of Zy-4 in a fuel bundle	2 kg
Exterior radius of Zy-4 tube	0.654 cm
Interior radius of Zy-4 tube	0.612 cm
Mass of colloidal graphite in a fuel bundle	5g

Table 22 Composition of Zy-4 (wt%)

Major elements (wt%)					
Sn	1.2 – 1.7				
Fe	0.07 – 0.20				
Cr	0.05 – 0.015				
Ni	0.03 – 0.08				
Zr	up to 100%				
Minor elements (wt%)					
Al	0.0075	H	0.0025	Si	0.0120
B	0.00005	Hf	0.0200	Na	0.0020
C	0.0270	Pb	0.0130	Ti	0.0050
Cd	0.00005	Mg	0.0020	W	0.0100
Co	0.0020	Mn	0.0050	U (total)	0.00035
Cu	0.0050	N	0.0080	U ⁻²³⁵	0.0000025

Neutronic calculations were carried out for burn up of 0 MWD/kgU and 6 MWD/kgU to get the neutron fluxes (Table 23) and from these data an average flux were calculated (4.5E+13

nv) to be used as input for the ORIGEN code. The values fluxes presented in Table 23 in red are for the neutron fluxes in the fuel while those in blue are for the neutron fluxes in the Zy-4. Also, using epithermal and fast neutron fluxes the spectral factors were computed on three groups by using the following relations:

$$\text{Therm} = (n/4T_o/T)^{1/2} \text{ for thermal } < 0.5\text{eV}$$

$$\text{Res} = 0.069 \text{ flux-res/flux-therm } < 1\text{MeV}$$

$$\text{Fast} = 1.45 \text{ flux-fast/flux-therm } < 15\text{MeV}$$

Table 23 Neutron fluxes (nv) in CANDU fuel for a burn up of 0.0 MWD/kg U and 6.0 MWD/kgU (in red: value for neutron flux in fuel; in blue: values for neutron flux in Zr-4)

Burn up = 0.0 MWD/kg U							
1.314E+12	7.743E+12	1.455E+13	1.813E+13	1.226E+12	7.218E+12	1.352E+13	1.673E+13
3.575E+12	2.101E+13	3.988E+13	5.418E+13	3.565E+12	2.095E+13	3.966E+13	5.364E+13
2.760E+12	1.713E+13	3.736E+13	6.537E+13	2.857E+12	1.773E+13	3.860E+13	6.730E+13
Burn up = 6.0 MWD/kg U							
1.749E+12	1.030E+13	1.936E+13	2.412E+13	1.632E+12	9.604E+12	1.799E+13	2.226E+13
4.760E+12	2.797E+13	5.305E+13	7.208E+13	4.748E+12	2.787E+13	5.277E+13	7.136E+13
3.660E+12	2.274E+13	4.961E+13	8.684E+13	3.789E+12	2.353E+13	5.126E+13	8.941E+13

Four cases were modelled by using the ORIGEN-S code, in order to see their impact on C-14 generation:

Case 1: all elements included

Case 2: N impurities were not considered

Case 3: C was not considered (CANLUB graphite and C as impurity in Zy-4)

Case 4: N and C were not considered

The results obtained for Case 1 and Case 2 are presented in Table 24. Particularly, the results obtained for C-14 are presented in Table 25 both as mass and as radioactivity.

Table 24 Calculated radionuclide concentrations in irradiated Zy-4 from CANDU fuel at a burn up of 6MWD/kg U

Radionuclide	Mass (g/kg of Zy-4)			
	Case 1		Case 2	
	charge	discharge	charge	discharge
B 10	9.26E-05	3.03E-07	9.26E-05	3.03E-07
B 11	4.07E-04	4.11E-04	4.07E-04	4.07E-04
C 12	2.24E+00	2.24E+00	2.24E+00	2.24E+00
C 13	2.73E-02	2.73E-02	2.73E-02	2.73E-02
C 14	0.00E+00	1.08E-04	0.00E+00	1.97E-07
N 14	3.98E-02	3.97E-02	0.00E+00	2.90E-11
N 15	1.57E-04	1.62E-04	0.00E+00	6.32E-09
O 16	1.30E+00	1.30E+00	1.30E+00	1.30E+00
O 17	5.25E-04	5.25E-04	5.25E-04	5.25E-04
O 18	2.98E-03	2.98E-03	2.98E-03	2.98E-03
F 19	0.00E+00	1.31E-09	0.00E+00	1.31E-09

Table 25 Calculated C-14 accumulated in irradiated Zy-4 from CANDU fuel at a burn up of 6MWD/kg U

C-14	Case 1		Case 2	
	g/kg of Zy-4	Bq/kg Zy-4	g/kg Zy-4	Bq/kg Zy-4
Discharge	1.08E-04	1.78E+07	1.97E-07	8.79E-07

The results obtained for Case 3 are very similar to those obtained for Case 1 while those obtained for Case 4 are similar with those resulted for Case 2. These data indicate that the carbon (both from colloidal graphite and from impurity in Zy-4) has low influence on the total C-14 generation in CANDU Zy-4 tubes.

2.7 RWMC contribution in WP3

RWMC contributed to D3.1 (issued in 2014). It is also in charge of D3.19 due in January 2017.

2.7.1 Distribution of ¹⁴C in irradiated cladding

A spent BWR fuel rod (STEP 1 type) located at the circumference of the assembly was obtained. The STEP I type fuel is an older fuel type in Japan that uses an 8×8 array in a lattice configuration. The average burnup was 39.4 GWd/tU for the fuel assembly and 41.6 GWd/tU for the fuel rod. After the fuel components were removed, the Zircaloy-2 claddings were washed with 6 M of HNO₃ in a warm bath and cut to an appropriate size. The thickness of the surface oxide layer was measured based on external observations. As shown in Figure 15, four types of samples were obtained for specific activity measurements of C-14. The external oxide layer of Zircaloy was peeled off through vertical compression of the columnar cladding (approximately 2 cm high) whose interior layer had previously been

removed. As a consequence, approximately 0.05 g of oxide was recovered as a powdery fragment.

The C-14 radioactivity in the cladding specimens was measured as follows: Firstly, the ring-shaped claddings and oxide samples were dissolved in an HNO₃ + HF solution with heating. Carbon components were evaporated by air bubbling for 30 min and oxidised by CuO in CO₂ at 1073 K. The material was then passed through three steps of a dry-ice cold trap to remove tritium and three steps of an alkaline trap (1 M of NaOH) to collect carbon dioxide (¹⁴CO₂). The potential contamination by radioiodine in a volatile state was removed by an AgI precipitation. The ¹⁴C radioactivity in the alkaline traps was measured by LSC (PerkinElmer Tri-Carb 2900TR).

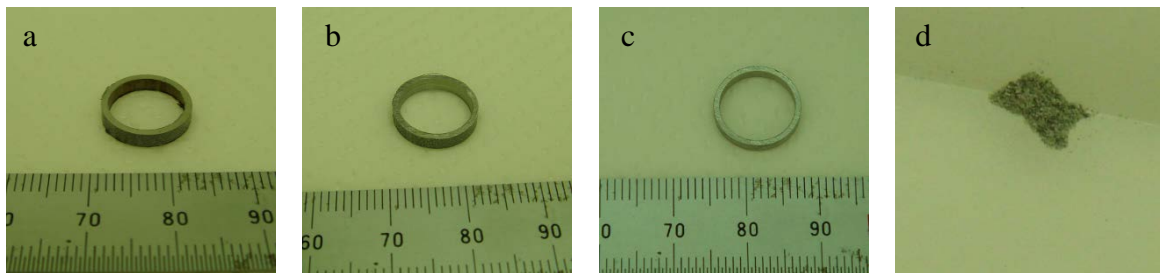


Figure 15 External appearance of irradiated claddings for ¹⁴C measurement: (a) with internal and external oxide layers in place, (b) with internal oxide removed, (c) with internal and external oxide removed, (d) (external) oxide fragment removed from the cladding [SAKURAGI, 2016].

Table 26 shows the results of ¹⁴C specific activity (Bq/g) for the irradiated cladding specimen shown in Figure 15. For the external oxide, units of grams in the specific activity of oxide are converted into grams of zirconium metal in order to facilitate comparison with the base metal. The average values of (a), (b), (c) and (d) are 1.49×10^4 , 1.53×10^4 , 1.49×10^4 and 4.04×10^4 Bq/g, respectively.

The radionuclides in cladding oxide are regarded as a source of instant release fraction (IRF) in the preliminary Japanese safety case, in which 20% of ¹⁴C in cladding was assumed as IRF and the remaining 80% was assumed as the corrosion-related congruent release from the base Zircaloy metal [FEPC, 2007]. In Table 26, the specific activity between oxide and base Zircaloy differs by a factor of 2.8. The ¹⁴C in Zircaloy is mainly generated from the

nitrogen impurity as a result of the $^{14}\text{N}(n,p)^{14}\text{C}$ reaction. Given that the nitrogen content in oxide and Zircaloy base metal are equal in amount, the activation calculation using the ORIGEN code suggests that the ^{14}C content in oxide is larger than the content in base Zircaloy metal due to the additional $^{17}\text{O}(n,\alpha)^{14}\text{C}$ reaction [SAKURAGI, 2013]. Based on the cladding geometry, thickness of the base metal and oxide layer (Table 27) and the density of Zircaloy and oxide layer, the abundance of ^{14}C in the oxide and the base Zircaloy can be estimated as 7.5% and 92.5%, respectively. This ^{14}C distribution corresponds roughly to the ^{14}C inventory in waste claddings estimated by the ORIGEN calculation described above, in which the respective percentages of 3.5% and 96.5% were suggested for the BWR STEP I cladding [SAKURAGI, 2013]. It can therefore be concluded from the results of both the measurements in this study and previous calculations that the assumption of 20% IRF in the safety case was somewhat conservative. However, the ^{14}C distribution in oxide for the PWR cladding was measured as 17% [YAMAGUCHI, 1999], which can be attributed to the oxide thickness of the claddings. In the literature, the oxide layer of PWR cladding is particularly thick (80 μm).

Table 26 Specific activity of ^{14}C for irradiated claddings and oxide [SAKURAGI, 2016].

Thickness (μm)		Specific activity (Bq/g)			
Base metal	Oxide layer	(a) Cladding with internal and external oxide	(b) Cladding with external oxide	(c) Cladding base metal	(d) External oxide*
		1.54×10^4	1.53×10^4	1.49×10^4	4.25×10^4
704.7	25.3	1.49×10^4		1.50×10^4	3.83×10^4
		1.43×10^4		1.47×10^4	

* Units of grams in the oxide are converted to grams of zirconium, not grams of ZrO_2 .

2.7.2 Released ^{14}C from irradiated cladding

The static leaching test was carried out using the irradiated Zircaloy-2 cladding, described above, with a 2 cm high cylinder (4.03 g) with only the external oxide layer (the internal oxide layer having been removed). Final polishing of the cladding interior was performed with a 0.02 mm abrasive. A glass vial with a simple cap was filled with 20 ml of diluted NaOH solution adjusted to a pH of 12.5. The solution was deoxygenated before use to achieve an initial ORP (oxidation-reduction potential) of -253 mV/SHE . The glass vial was

placed inside a stainless steel container and sealed by gasket to maintain the initial inert condition and to prevent leakage of volatile ^{14}C . This immersion procedure was carried out under nitrogen atmosphere inside a glove box. The experimental setup of the leaching test is shown in Figure 16.

After 6.5 years of immersion at room temperature (approximately 293 K), the outer and inner vessels were opened in a glove bag with a vacuum tube attached. The gaseous ^{14}C was collected through the tube by using the three steps of an alkaline trap after passing through an oxidation furnace. A portion of the liquid phase was provided for measurement of total dissolved ^{14}C and dissolved organic and inorganic ^{14}C . In the total ^{14}C measurement, an aliquot of leachate was mixed with a carrier carbon (Na_2CO_3 and $\text{C}_2\text{H}_5\text{OH}$), an oxidant (potassium persulfate, $\text{K}_2\text{S}_2\text{O}_8$), a catalyst (AgNO_3), and an acid (H_2SO_4) in a warm vessel. In the organic / inorganic separation method, the inorganic ^{14}C was fractionated from another aliquot by bubbling for 30 minutes under acidification. Then, the remaining organics were oxidised with the same reagents used for total ^{14}C measurement and the volatile ^{14}C ($^{14}\text{CO}_2$) was collected by an alkaline trap in the same manner as described for total ^{14}C measurement. Leached ^{14}C in the alkaline traps was measured by a liquid scintillation counter (PerkinElmer Tri-Carb 3100TR).



Figure 16 External view of outer vessel (left) and cladding immersed in glass vessel (right) for long-term static leaching test.

Table 27 shows the results of the leached amount of ^{14}C for the respective fractions after 6.5 years of aqueous immersion. The gaseous released ^{14}C (0.317 Bq) is less than the dissolved ^{14}C species (2.00 Bq in total fraction). The sum of the dissolved inorganic and organic ^{14}C is 1.64 Bq, which corresponds roughly to the total dissolved ^{14}C . The leached organic ^{14}C in solution is 3 times the amount of the inorganic ^{14}C .

The leaching ratio is shown in Figure 17. It is equivalent to the leached amount (gaseous + dissolved) divided by the initial inventory, and is less than 3.8×10^{-5} . It is consistent with the previous short-term leaching tests, described above, involving PWRs or BWRs STEP III claddings [YAMAGUCHI, 1999] [YAMASHITA, 2014], which showed small ^{14}C leaching ratios.

Table 27 Results of released ¹⁴C in different fractions after 6.5 years aqueous immersion, in Bq [SAKURAGI, 2016].

Initial inventory, $A_{\text{inventory}}$	Gas phase	Total dissolved	Dissolved inorganic	Dissolved organic
6.17×10^4	0.317	2.00	0.403	1.24

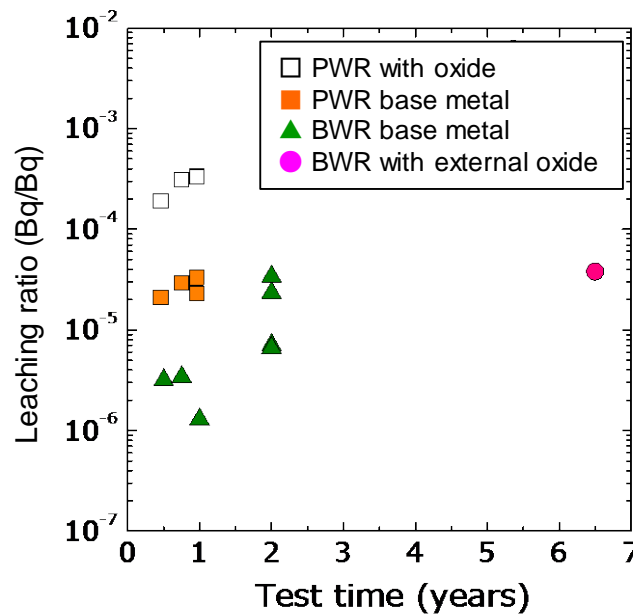


Figure 17 Leached ¹⁴C from irradiated claddings. PWR with oxide [YAMAGUCHI, 2014], PWR without oxide [YAMAGUCHI, 2014], BWR without oxide [YAMASHITA, 2014], and BWR with external oxide [SAKURAGI, 2016].

The following is an examination of which part of the irradiated cladding is the source of the leaching source of ¹⁴C based on the assumption that the radionuclide release from the Zircaloy matrix is regarded as a corrosion-related congruent release. The immersed cladding in this study comprises the external oxide layer and the bare Zircaloy metal inside the tube. Therefore, the potential leaching source can be from three surfaces: (a) interior bare Zircaloy (r_{in-Zry}), (b) external Zircaloy and oxide interface ($r_{out-Zry}$), and (c) external oxide layer ($r_{out-oxide}$). The ¹⁴C released from the oxide layer can be expressed from the total release of ¹⁴C (r_{total}) obtained by experiment, as:

$$r_{out-oxide} = r_{total} - r_{in-Zry} - r_{out-Zry} \quad (1)$$

The matrix corrosion rate was obtained from out-of-pile study in the temperature range of approximately 561 K to 673 K [HILLNER, 1977]. Here, the pre-transition cubic rate constant, k_C , is applied to the inside bare Zircaloy (r_{in-Zry}) and the post-transition linear rate constant, k_L , is applied to the external Zircaloy ($r_{out-Zry}$) because the corrosion kinetics of Zircaloy follows a cubic rate law before transition (“breakaway”), and then, once corrosion has progressed for 1 or 2 μm , the corrosion kinetics changes linearly with time [HILLNER, 1977]. The details are described elsewhere [SAKURAGI, 2016].

Figure 18 shows the estimated release ratios from the possible source surfaces at 293 K and 6.5 years of immersion. Due to the low corrosion rate of Zircaloy, especially the extremely slow post-transition corrosion, the leached ^{14}C from Zircaloy is negligible. This leads to the conclusion that the main source of ^{14}C release is the oxide. By applying the concept of a corrosion-related congruent release described above, the ^{14}C release from the oxide layer is almost 100% of the amount in the previous short-term PWR test [YAMAGUCHI, 2014], for which the cladding has both post-transition internal and external oxide layers of 10 μm and 80 μm respectively.

In conclusion, the oxide layer is dominant in the ^{14}C release from irradiated cladding. However, regarding the ^{14}C in oxide as IRF would be too conservative because the released ^{14}C is less than 0.01% of the total after 6.5 years of immersion. Both the low amount of ^{14}C in oxide and the low leaching rate indicate that the ^{14}C in oxide does not have a major impact on the instant release fraction in the safety case.

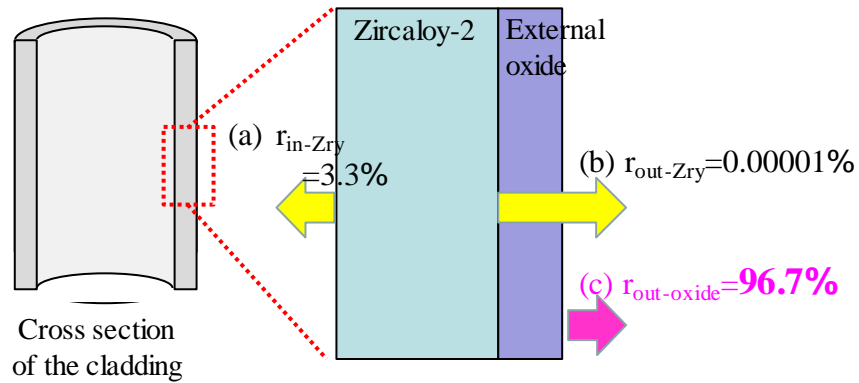


Figure 18 Estimated leached ¹⁴C from oxide based on the corrosion-related congruent release.

2.7.3 Acknowledgement

This research is a part of the “Research and development of processing and disposal technique for TRU waste (FY2015)” program funded by Agency for Natural Resources and Energy, Ministry of Economy, Trade and Industry of Japan.

2.8 SCK.CEN contribution in WP3

In 2016, SCK.CEN was in charge of D3.12 in Task 3.3, entitled “3rd year progress report”. This deliverable consists of describing a complete material characterisation on unirradiated Zr-4, as well as the experimental setups for corrosion rate measurements and C-14 speciation. Within WP3, SCK-CEN is in charge of four deliverables; D3.4 (issued in 2014), D3.10 (issued in 2015), D3.12 (submitted in June 2016), and D3.17 (due in 2017).

2.8.1 Materials

Metallographic characterisation of unirradiated Zr-4 was performed. Figure 19 presents the grain structure observed with a scanning electron microscope (SEM) in BSE mode. The grain size number was estimated at 11.8, which corresponds to an average grain diameter of 6 μm and surface of 36.4 μm^2 . The small black spots can be attributed to $\text{Zr}(\text{Fe},\text{Cr})_2$ Laves phases.

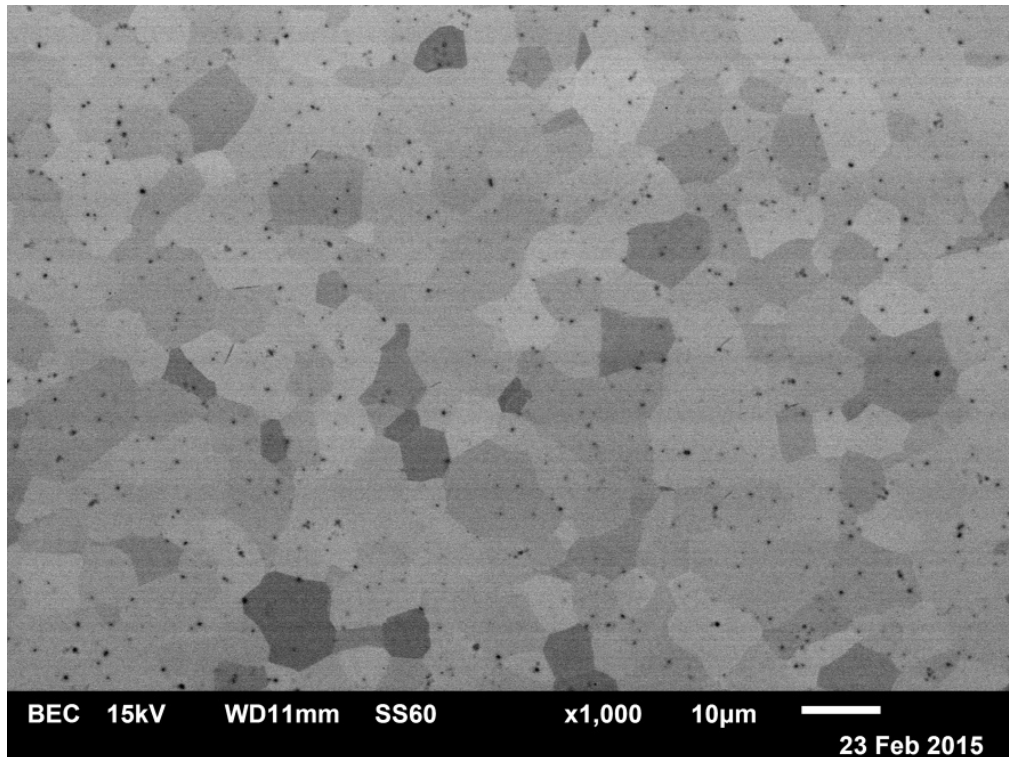


Figure 19 SEM image (BSE mode) revealing the grain structure of an unirradiated Zr-4.

Typical images of the defect structure of Zr-4 is shown in Figure 20. The main defects are line dislocations with a density of $4.1 \times 10^{13} / \text{m}^2$. The grain orientation can be determined from the diffraction pattern as shown in Figure 20. Most grains have a comparable orientation following the [1-210] zone axis. During the manufacturing process the grains become textured, which results in grains having a similar orientation.

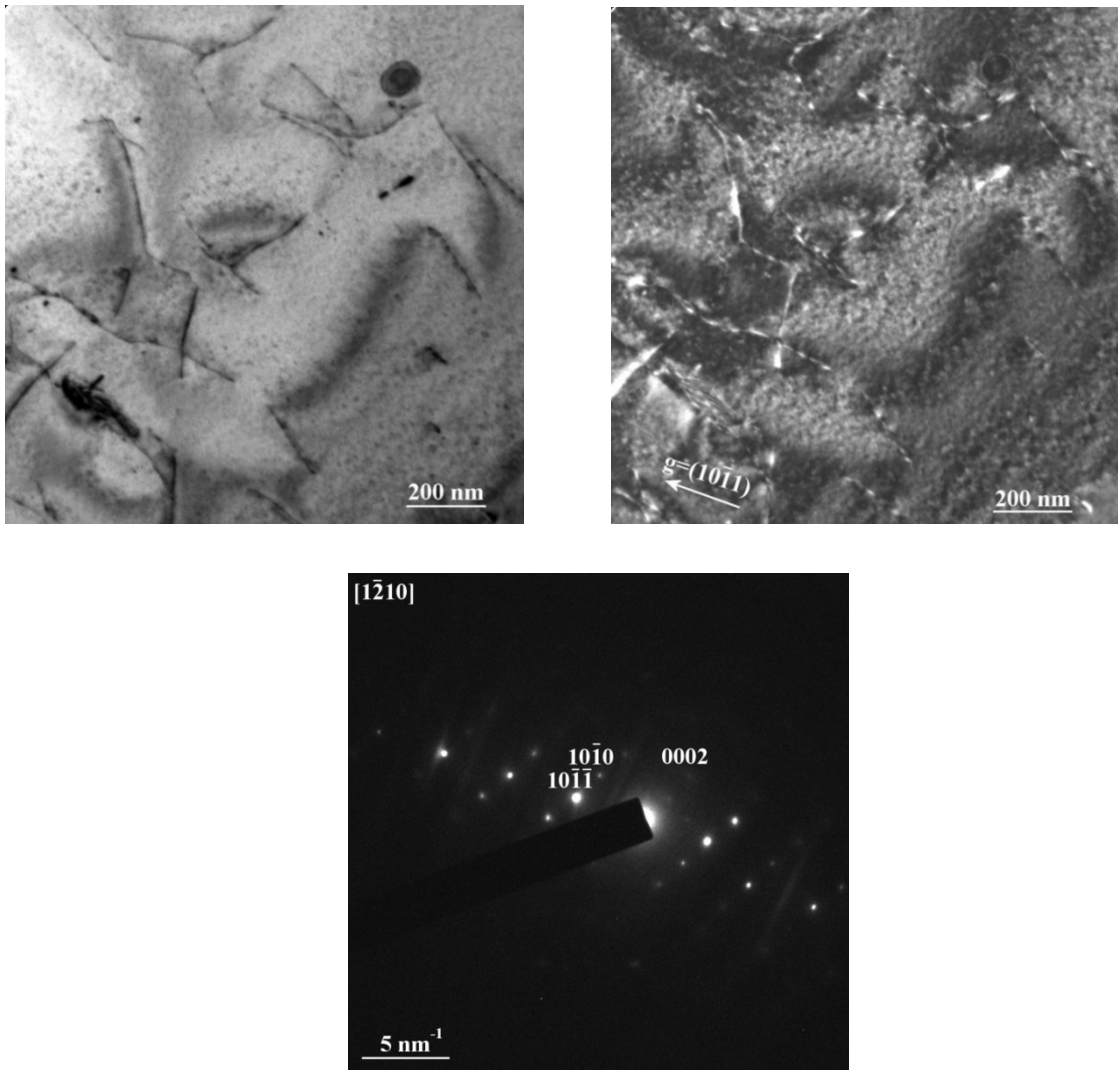


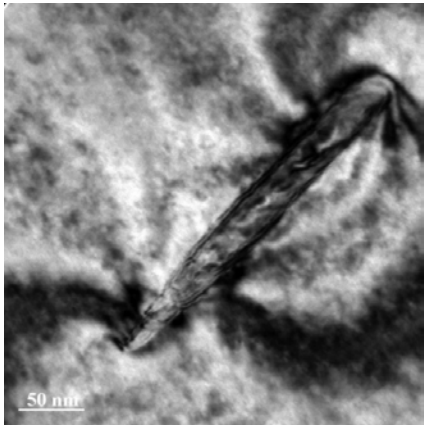
Figure 20 Top left: Bright field; Top right: dark field image of the typical defect structure in unirradiated Zr-4; Bottom: Typical diffraction pattern showing the grain orientation following the [1-210] zone axis.

Most precipitates present in Zr-4 are Laves phases with a nominal composition of $Zr(Fe,Cr)_2$. The composition is confirmed by the EDS analysis on this particle. Apart from the Zr signal, peaks corresponding to Fe and Cr were measured as well. Carbon is considered to result from surface contamination during the analysis as it was not initially present in this sample.

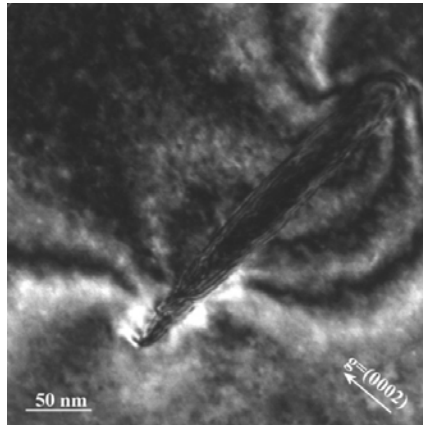
Figure 21 shows a second type of precipitate. The bright and dark field images show that these precipitates are elongated along the (0002) planes with needle or platelet shapes. The EDS spectrum in Figure 21 e) shows the composition of the precipitate in comparison to the bulk material of Zr-4. For a better visual comparison, the spectrum was renormalized so

that both spectra have the same total number of counts. The bulk metal is mainly Zr. Small amounts of C and O were detected as well, which can be attributed to the expected contamination of the surface and a slight oxidation of Zr, which is very reactive. When magnifying the spectrum between 2 and 6 keV, a small Sn peak could be found, in agreement with the 1.2wt% of Sn added to Zr-4. Cr and Fe were not detected in the bulk as they contribute to the formation of Laves phases. The spectrum of the precipitate contains only Fe and C. The C content is significantly higher in the precipitate compared to the bulk material. This may result from higher local contamination while recording the spectrum or it can be an indication that carbon is present in the precipitate.

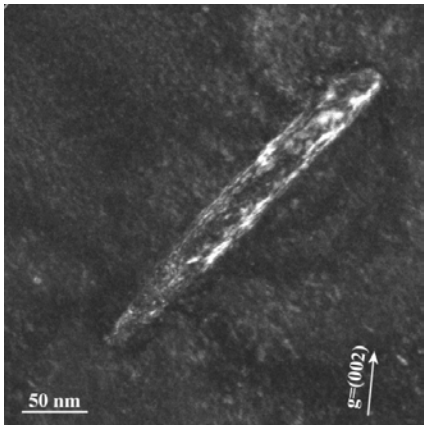
Crystallographic structure can help identify the precipitate from the diffraction pattern (Figure 21 d). Because of the small size of the precipitate, the appearance of diffraction spots from the bulk Zircaloy could not be avoided and the 0002, -1011 and -1010 reflections, typical for the [1-210] zone, are also indicated. The additional reflections agree with the [110] zone axis of a face centred cubic (FCC) structure with a lattice parameter of $4.6 \pm 0.2 \text{ \AA}$. Several phases, including ZrC, ZrN or ZrH₂, were found to have the right crystal structure. In combination with the EDS results, it is most likely that this phase is a ZrC precipitate.



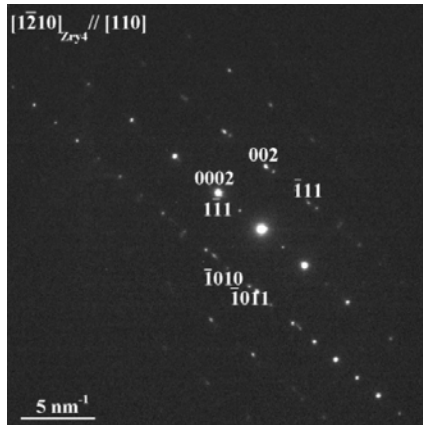
a)



b)



c)



d)

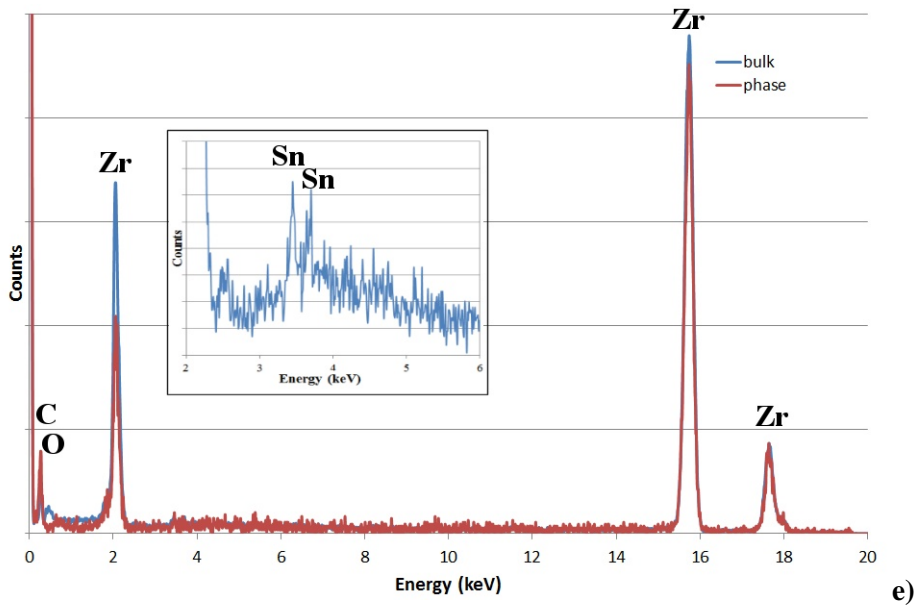


Figure 21 a) bright field and b,c) dark field images of a second type of precipitate in Zr-4, presumably a ZrC. d) The corresponding diffraction pattern and e) the EDS analysis. The inset shows a magnified part of the bulk metal spectrum, clarifying the presence of Sn peaks.

2.8.2 Corrosion test

Two types of corrosion tests have been performed by SCK.CEN:

- Static corrosion tests to allow for a more realistic corrosion behaviour and measure the resulting released ^{14}C and its speciation
- Accelerated corrosion tests involving polarisation, which mainly serve for preliminary speciation determination.

2.8.2.1 Static tests

Figure 22 shows the experimental setup of a static corrosion test. It consists of a PEEK-coated steel vessel with an internal volume of 50 cm³. The vessel is filled with a Ca(OH)₂ solution at pH 12.5 in which a Zr-4 sample (irradiated or unirradiated) is immersed. Tests will be run for a period of 6 months. After the test, both liquid and gaseous samples will be analysed by gas chromatography (GC).

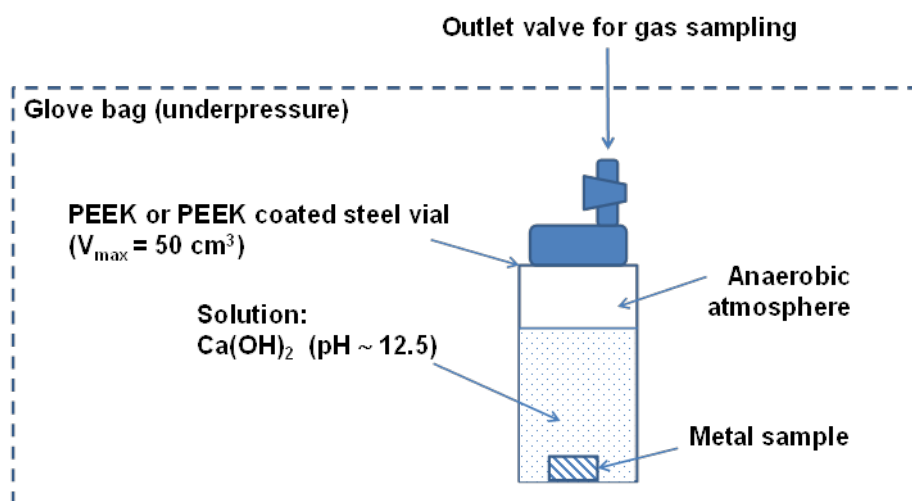


Figure 22 Experimental setup of the static corrosion tests performed at SCK.CEN.

2.8.2.2 Polarised corrosion tests

Figure 23 shows the experimental setup of a polarised corrosion test. A three-electrode cell is used, including a working electrode (Zr-4), a house-made Ag/AgCl reference electrode, and a platinum counter electrode. During preliminary tests, potentiodynamic polarization measurements have been carried out by applying a potential range from the cathodic to the anodic region. The resulting current density was recorded. A representative I-E polarization curve, showing a broad passive range is presented in Figure 24.

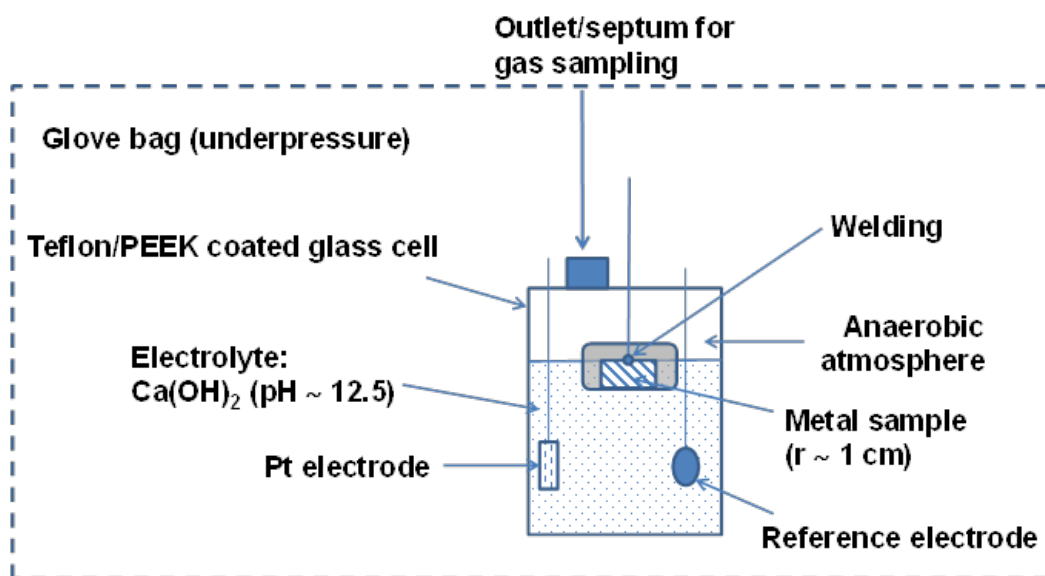


Figure 23 Experimental setup of a polarised corrosion test.

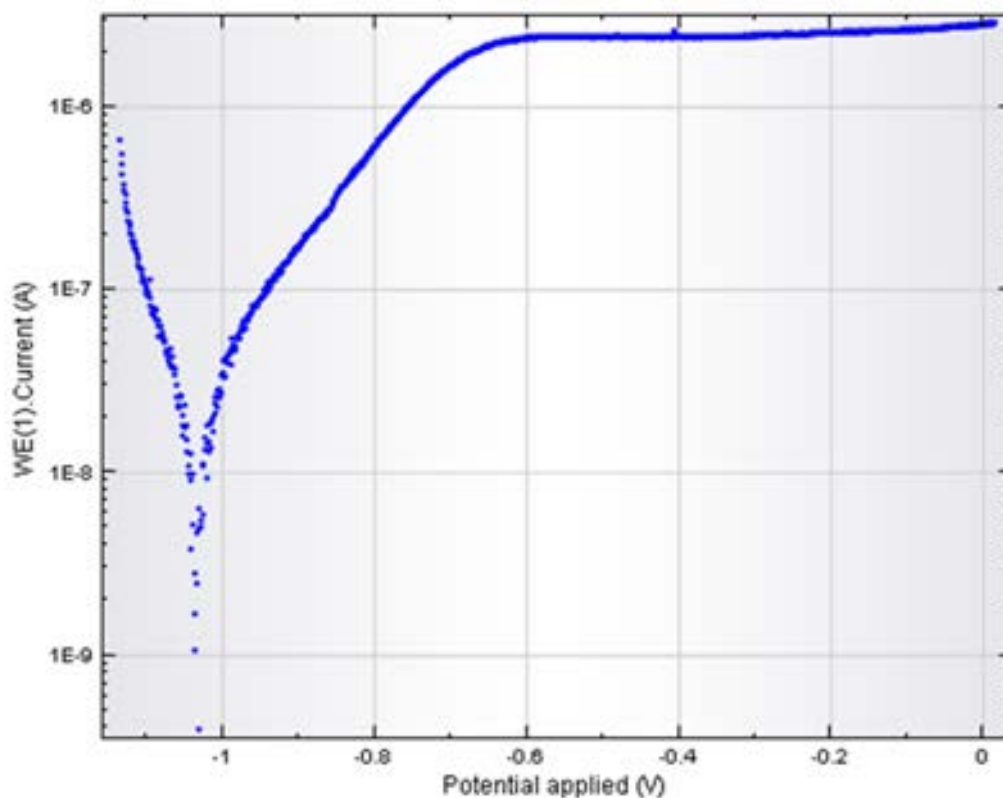


Figure 24 I-E Polarization curve of unirradiated Zr in a solution of $\text{Ca}(\text{OH})_2$ at pH 12.5.

2.8.3 Gas chromatography

To determine ^{14}C speciation released from Zr-4 in $\text{Ca}(\text{OH})_2$, a GC system will be installed by the end of 2016. The acquired system is a Shimadzu GC-2010 Plus, which is tailor-made to meet the requirements of the CAST project. Detectors include a Flame Ionization Detector (FID), a Barrier Discharge Ionization Detector (BID), and a Pulse Discharge Helium Ionisation Detector (PDHID). The detection limit of the PDHID detector is 50 ppb (ng/l).

3 Summary

3.1 Introduction

During the third year of the CAST project, WP3 participants have worked on Tasks 3.2 and 3.3. The leaching and corrosion experiments have been launched by most participants on both irradiated and unirradiated materials. However, the experimental setups have taken more time than initially planned. Therefore, the coordinator has been informed that an extension of 3 months will be required to complete the objectives of CAST WP3. This will be discussed for agreement at the October 2016 General Assembly Meeting.

Table 28 presents the contributions of the partners involved in WP3.

Table 28 Contributions of the different partners

Organisations	Andra	CEA /AREVA	RATEN ICN	JRC	KIT	RWMC	SCK-CEN	Subatech
Task 3.1 – State of the art	x					x		
Task 3.2 – Development of analytical methods		x		x	x	x		x
Task 3.3 – Characterisation of ¹⁴ C released		x	x	x	x	x	x	x
Inventory			x		x	x	x	x
Corrosion rate			x	x		x	x	
Liquid phase		x	x	x	x	x	x	x
Gas phase			x	x	x	x	x	
Task 3.4 – Synthesis / interpretation	x	x	x	x	x	x	x	x
Total person-months per participant	7+2	31	33	15	30	23	21	25

The following sections present a summary of the work to date.

3.2 Task 3.1

Task 3.1 was devoted to the State of the Art on C-14 release from Zircaloy and Zr alloys under repository conditions. D3.1, issued in 2014, is a part of this Task [GRAS, 2014]. It highlights some outstanding issues, which are essentially taken into consideration in WP3:

- Inventory of ¹⁴C
 - Comparison between modelling and measurements

- ¹⁴C speciation into the metal and oxide layers
- Corrosion of Zircaloy at low temperatures
 - Regime of corrosion for oxide thickness (t_{ox}) \gg 2.5 μ m
 - Consequences of the dense surface layer of hydrides (hydrogen pick-up ratio \sim 90 %).¹
 - Low dissolution rate of ZrO₂ layers in alkaline solutions in the presence of any complexing species (in relationship with the chemistry of disposal sites' groundwater)¹
- Leaching
 - Feedback of reprocessing plants (e.g. leaching of claddings in pools)¹
 - Chemical forms of released ¹⁴C
 - Rates of release of ¹⁴C

3.1 Tasks 3.2 and 3.3

3.1.1 Materials

Table 29 and Table 30 summarise, respectively, the unirradiated and irradiated materials available for use in WP3. These materials have been considered for the leaching and corrosion experiments in alkaline media involved in Tasks 3.2 and 3.3. Analyses have been conducted on liquid and / or gas samples. The determination of the inventory and speciation of C-14 released from Zircaloy in alkaline conditions is in progress. Zircaloy-2, Zircaloy-4 and M5TM materials were available for the CAST project. The different suppliers are European and Japanese, which allows a variety in terms of history of the materials and conditions in nuclear power plants. For most materials, the nitrogen content has been

¹ Not studied in CAST

determined experimentally. Metallography has been carried out to identify the microstructure of the materials, both irradiated and unirradiated. Knowing that the dissolution of zirconia is involved in C-14 release, the thickness, properties and microstructure of zirconia has been investigated for irradiated materials. From a corrosion point of view, unirradiated materials are also studied as they allow further investigation on the corrosion kinetics for different oxide thickness, especially above 2 μm to study the post-transition kinetics. The cleaning of the samples has been minimised in order to be representative of the disposal conditions. Therefore, for unirradiated materials, cleaning with ethanol followed by rinsing with water and air drying was generally performed. Regarding irradiated materials, rinsing in HNO_3 was carried out on spent fuel hulls (which contains other radioelements), followed by rinsing with water and air drying.

Table 29 Unirradiated materials.

Participants	Zr alloys types	Chemical composition (real N)	Metallography	Pre-treatment of the surface specimen	Oxide thickness (µm)
ITU/JRC	Zr-4	30-40 ppm	To be done	As-received	~ 3
RATEN ICN (ex. INR)	Zr-4	10 ppm	OM, SEM	Oxidation	1.7 – 2.7
RWMC	Zr-4 (plate), Zr-2, Zr	28 ppm 32ppm 10ppm	OM, SEM	Cold-rolling, and vacuum annealing Surface condition: alumina powder polishing (0.02 mm)	0.005 – 0.02
	Zr-4 (tube)	30ppm	OM, SEM <i>Mean Diameter of intermetallic compound: 0.16µm (outer side)</i>	As-received	~ 0.005 (naturally formed in air)
SCK.CEN	Zr-4	17 – 25 ppm	OM, SEM TEM	As-received	naturally formed in air

Table 30 Irradiated materials.

Participants	Zr alloys types	Chemical composition (real N)	Microstructure	Activation history (known)	¹⁴ C Inventory (Bq/g)	Pre-treatment of specimen, i.e. surface condition etc.
Areva	Supply the materials to CEA					
CEA	M5 TM Zr4 (inner layer) Zr-0.8%Sn (outer layer) Tube shape	27 ppm (estimated) 34 ppm (estimated)	OM (planned)	46.570 GWd/tHM / 54.500 GWd/tHM	Modelling in progress (Round Robin test)	Industrial treatment (shearing, fuel dissolution in boiling HNO ₃ , rinsing)
ITU/JRC	Zr-4 with Zr-2.5Nb (external cladding) Ring shape	30 – 40 ppm	OM + SEM (planned)	Max 100.5GWd/tHM	1.3 x 10 ⁴	Acid cleaning with HNO ₃ and/or 15% H ₂ SO ₄ (depending on their original location) + water and drying in air
KIT	Zr-4 + Zr-	Nominal:	OM	50.4	Calculated:	wash cycle

	0.8%Sn (outer layer) Ring shape	50 ppm		GWd/tHM	3.2(±0.3)×10 ⁴ Experimental: 3.7(±0.4)×10 ⁴	with ultrapur e water / ultrasoni c bath
RATEN ICN (ex. INR)	Zr-4 Tube shape	30 ppm	OM	7.5GWday/tH M	1.776 x 10 ⁴	spent fuel dissoluti on using HNO ₃ ; rinsing with pure water
RWMC	Zr-2 STEP3	Not available	OM	39.7 GWd/tHM 3 cycles	Metal ; 1.74 x10 ⁴	Polishin g and rinsing with pure water, (remova l of the oxide layer)
	Zr-2 STEP1	Not available	OM	41.6 GWd/tHM 5 cycles	Metal ; 2.48 x10 ⁴	Polishin g and rinsing with pure water, (remova l of the oxide layer)
	Zr-2 STEP 1	Not available	OM	40.4 34.2 41.6	Metal + outer oxide film; 3.57x10 ⁴ , 1.53 x10 ⁴ 3.42 x10 ⁴	Polishin g inner surface and rinsing with pure water. (samples with oxide outer layer)
	Zr-2	Not	OM		Oxide (outer	Remove

	STEP 1	available		34.2 41.6 37.4	layer) 4.04 x10 ⁴ 5.69 x10 ⁴ 5.82 x10 ⁴ (Bq/gr)* *Bq/gr is in terms of Zr metal weight	d from Zr-2 tube
SCK-CEN	Zr-4	17-25 ppm (measured)	OM + TEM	49 GWd/tHM	Calculated: 1.33 x10 ⁴ 1.95 x10 ⁴	Rinsing with water + drying in air
Subatech/Armines	M5 + Zr-4 (Identical to CEA)					

3.1.2 Task 3.2

Task 3.2 is devoted to the analytical development based on the needs highlighted in Task 3.1. The main contributors to this task are CEA, KIT and Subatech / Armines who are responsible for D3.3, D3.7 and D3.9 respectively. JRC / ITU, RATEN ICN, RWMC and SCK.CEN are also involved at a lower level. In 2016, Subatech submitted the D3.9 deliverable describing the analytical strategy to measure C-14 organic molecules in NaOH solution containing irradiated Zircaloy.

Overall, CEA and Subatech have been working in alkaline solution and confirmed that inorganic / organic partition can be determined by LSC after 14 days of immersion. By contrast, C-14 speciation requires AMS as the released C-14 is below the detection limit of LSC.

Subatech have proposed an analytical strategy for the analysis of C-14 carboxylic acids released from irradiated Zircaloy (WP3) and steels (WP2). This strategy is based on the use of IC for separation of carboxylic acids and LSC for the quantification of C-14 in the IC collected fractions. The proposed method is based on the use of K₂[CuFe(CN)₆] without binding polymer resin characterized by its selectivity for the identified radionuclides and the absence of interaction with target C-14 carboxylic acids. However, the experimental protocol combining IC and LSC further to filtration and resin treatment stages of the

leaching solution shows that the C-14 carboxylic acid activities are below the quantification limits of LSC i.e. 0.04 Bq/mL and that AMS, a more sensitive technique, will be required to determine C-14 in the chromatographic fractions.

KIT has been working in acid solution to determine C-14 inventory as well as the gaseous / aqueous partition. Using the C-14 separation and analysis techniques developed in WP3 for gaseous and aqueous samples derived from acid digestion of irradiated Zircaloy-4 specimens, it was possible to quantify the C-14 content in these samples. Furthermore, the partitioning of C-14 between inorganic and organic C-14 bearing compounds and their distribution between solution and gas phase was investigated. In addition to C-14, the contents of Fe-55, Sb-125 and Cs-137 in irradiated Zircaloy-4 were analysed and also compared to MCNP-X calculations.

Table 31 summarises the analytical development in WP3.

Table 31 Analytical development.

Participants	Sampling (gas/liquid)	C-14 speciation	Techniques	Aims
CEA	Liquid	yes	TC analyser (TIC + TOC) LSC + AMS IR IC GC-MS ESI – MS	Total Carbon Quantification of C-14 Speciation (organic molecules) Quantification of carboxylic acids Low molecular weight molecules High molecular weight
ITU/JRC	Gas and liquid	Only gas /liquid phase separation	LSC ICP-MS GC-MS	TIC-14/TOC-14
KIT	Gas and liquid	yes	LSC ICP-MS GC-MS α - γ -spectrometry	TIC-14/TOC-14 Inventory + partition Activity
RATEN ICN	Liquid	Only inorganic/organic partition	LSC	TIC-14/TOC-14
RWMC	Gas and liquid	yes	LSC γ -spectrometry IC-MS	Partition Activity Organic/Inorganic
SCK-CEN	Gas and liquid	yes	γ -spectrometry LSC / AMS TOC GC IC	Activity Inventory Speciation
Subatech / Armines	Liquid	yes	LSC + AMS IC	TIC-14/TOC-14 Speciation

3.1.3 Task 3.3

This task involves 15 deliverables (D3.2, D3.4-6, and D3.8-19). In 2016, the activities have been focused on launching the leaching experiments in alkaline solutions and start C-14 measurements in terms of inventory and speciation. Following the progress meeting held in Madrid on 1-2 June 2016, the planning for the leaching experiments and subsequent corrosion measurements will have to be adjusted to meet the requirements of the CAST project. Indeed, the purchase of the equipment, as well as the time required for the experimental setups delayed the launch of most leaching experiments. The deliverables due by February 2017 (D3.14-D3.19) will have to be postponed. According to the experience of

RWMC, 6 months is a reasonable duration to run the leaching experiment and measure released C-14, therefore an extension of three months is necessary to achieve the objectives of WP3.

Table 32 and Table 33 summarise the conditions for the leaching experiments in WP3 for irradiated and unirradiated materials.

Surface characterisations, including internal and external oxide layers observations by using scanning electron microscopy (SEM) and transmission electron microscopy (TEM), have been conducted prior to running the leaching experiments. Additional surface characterisations will be carried out following the leaching experiments to identify the impact of corrosion and dissolution of Zirconia.

To measure the corrosion rate (CR), specific experiments have been considered involving electrochemical measurements to determine the polarisation resistance (R_p) by using the linear polarisation resistance (LPR) technique. Moreover, Co^{60} counting is also carried out for the leaching experiment, which gives an estimation of the corrosion rate.

Table 34 and Table 35 summarise the current corrosion experiments carried out in WP3 for irradiated and unirradiated materials.

The results obtained during 2016 in terms of CR are summarised in Table 36 and Table 37. The current results on C-14 analyses (inventory and speciation) are summarised in Table 38.

KIT has shown that in acid solution, the vast majority of C-14 released from irradiated Zircaloy-4 is present as hydrocarbons into the gas phase (about 88%) and aqueous phase (> 11%). Almost no (< 1%) inorganic C-14 bearing compounds (e.g. carbonates, bicarbonates) were found in all experiments (glass reactor as well as autoclave) conducted with irradiated Zircaloy-4. Also remarkable is the similar ratio between inorganic and organic C-14 bearing compounds in the aqueous phase (1:390) and gas phase (1:430).

The comparison of experimental and theoretically predicted contents of various radionuclides (C-14, Fe-55, and Sb-125) and their good agreement further prove the reliability of the obtained data. The experimentally determined activities of the activation products in the irradiated Zircaloy-4 agrees within a factor < 2 with the MCNP-X

calculation, except for the fission product Cs-137. The difference is considered as relatively small taking into account the limited availability of data for the calculations.

Despite extensive testing of the separation technique by dissolving non-irradiated Zircaloy, the interference of gaseous HT, quantitatively released from irradiated Zircaloy-4 during digestion, and its oxidation to HTO was not taken into account and modifications of the separation technique were necessary.

Although the digestion experiments were performed under acidic conditions, clearly outside of repository-relevant conditions, little impact on the chemical form of C-14 released from irradiated Zircaloy under repository relevant conditions is expected.

RWMC performed leaching experiments over 6.5 years on Zr-2 and Zr-4 hulls in NaOH solution at pH 12 under deaerated conditions. The experiments were performed on materials exempt of oxide layers in order to determine the released C-14 fraction. According to their results, most C-14 is released by the oxide. In addition, the estimation of an instant release fraction (IRF) of 20%, considered from a safety assessment point of view, is far too conservative. Investigation on the dissolution rate of zirconia in alkaline media should be conducted.

Table 32 Leaching conditions for irradiated materials

Participants	Porewater	pH	Temperature	O ₂ measured	Duration
CEA	NaOH	12	~30°C	no	14 days -5.5 months
ITU/JRC	NaOH	~12 (not buffered)	30°C 80°C (possibly)	No	3 months
KIT	H ₂ SO ₄ /HF	1-3	ambient	not applicable due to argon / hydrogen overpressure	30 min – 6 hours
RATEN ICN	NaOH	12.5	Room temperature	Monitoring of the O ₂ content will be attempted	3 months 6 months 1 year
RWMC	NaOH	12.5	Room temperature	Eh < -250 mV Calculated by ORP	10 years (max)
SCK-CEN	Ca(OH) ₂	12.5	ambient	no	6 months
Subatech/Armines (CEA experiment)	NaOH	12	30°C	no	14 days 5.5 months

Table 33 Leaching solution for unirradiated materials

Participants	Porewater	pH	Temperature	O ₂ measured	Duration
ITU/JRC	NaOH	~12 (not buffered)	30°C	No	~3 months
RATEN ICN	NaOH	12.5	Ambient 80°C	O ₂ measurements	3 months 6 months
RWMC	pure water, NaOH, Ca(OH) ₂ ,	7 – 8 12.5	30°C, 50°C, 80°C 160°C	< 0.1 ppm	1 - 60 months
	pure water	7 - 8	180°C, 270°C	< 8ppm	up to 200days (30days interval)
SCK.CEN	Ca(OH) ₂	12	Ambient	no	3 months

Table 34 Corrosion experiments for irradiated materials

Participants	Corrosion rate
ITU/JRC	Co ⁶⁰ counting
RATEN ICN	Co ⁶⁰ counting + LPR
RWMC	Estimated by C-14 released fraction
SCK-CEN	LPR

Table 35 Corrosion experiment for unirradiated materials

Participants	Corrosion rate
SCK-CEN	LPR
ITU/JRC	Possible (from H ₂ measurements)
RWMC	H ₂ measurements
RATEN ICN	LPR

Table 36 Current results for corrosion rate (CR) measurements on irradiated materials in alkaline solutions

Participants	Materials	Solution	CR (nm/yr)
SCK-CEN	Zr-4	Ca(OH) ₂	To be determined
ITU/JRC	Zr-4	NaOH	To be determined
RWMC	Zr-2 Zr-4	NaOH	~10
RATEN ICN	Zr-4	NaOH	To be determined

Table 37 Current results for corrosion rate (CR) measurements on unirradiated materials in alkaline solutions under deaerated conditions at room temperature.

Participants	Materials	Solution	CR (nm/yr)
RATEN ICN	Zr-4	NaOH	3 – 480 (LPR)
RWMC	Zr-2	NaOH	~ 5 (H ₂ measurements)
	Zr-4		
SCK-CEN	Zr-4	Ca(OH) ₂	To be determined

Table 38 Current results on C-14 analyses (inventory + leached in NaOH solution).

Participants	Electrolyte	Temperature	Duration	Materials	C-14 Bq/gr	Inorganic Bq/gr	Organic Bq/gr
KIT	H ₂ SO ₄ /HF (30°C) pH 1-3	30°C	30 min 5 hours	Zr-4	Calculated Inventory : 3.2(±0.3)×10 ⁴ Experimental Inventory: 3.7(±0.4)×10 ⁴	Liquid: 1.0(±0.1)×10 ¹ Gas: 7.2(±0.7)×10 ¹	Liquid: 4.0 (±0.4)×10 ³ (11.4%) Gas: 3.1(±0.3)×10 ⁴ (88.4%)
RWMC	NaOH pH 12.5	25°C	1-5 years	Zr-2	0.007 – 0.1815 Bq/gr of solution	0.0047 – 0.0153 Bq/gr of solution (18 – 73%)	0.0017 – 0.0357 Bq/gr of solution (27 – 82%)
CEA	NaOH pH 12	30°C	14 days	M5 TM	6.1 ± 0,5 (solution)	3.3 ± 0,4 (solution)	2.8± 0,4 (solution)
RATEN ICN	-	Ambient	-	CANDU	Calculated inventory: 1.776 x 10 ⁴	-	-
JRC / ITU	-	Ambient	-	Zr-4	Calculated inventory: 1.3 x 10 ⁴	-	-

4 Conclusions and perspectives

In 2016, WP3 activities have focused on Tasks 3.2 and 3.3; aiming towards the analytical development, C-14 analyses and corrosion rate measurements from irradiated Zircalloys in disposal conditions.

Three deliverables (D3.9, D3.12 and D3.13) have been submitted to the coordinator for review.

Most participants have finalised their experimental setup for the leaching and corrosion experiments. Leaching experiments on irradiated materials have been launched and corrosion rates have been measured using different techniques. However, the experiments on irradiated materials have been delayed for several groups. Some results are already available in terms of C-14 inventory and / or corrosion rate measurements in H₂SO₄/HF, NaOH (pH 12), Ca(OH)₂ (pH 12) and pure water for irradiated Zr-2 and Zr-4. Modelling will be performed by Nagra to determine C-14 inventories on the available materials in WP3. The interested groups will supply Nagra with the required data (N content, location of the cladding, geometry...) for modelling.

2017 will be devoted to the completion of Tasks 3.3 and 3.4.

A joint technical WP2&3 progress meeting will be held on 25 October 2016 to discuss the ongoing work.

References

ALLIOT C., AUDOUIN N., BONRAISIN A.C., BOSSÉ V., LAIZÉ J., BOURDEAU C., MOKILI B.M., MICHEL N., HADDAD F. [2013]. ⁸²Sr purification procedure using Chelex-100 resin. *Applied Radiation and Isotopes*. 74, p56–60.

Bahri M., Suzuki-Muresan T., Landesman C., Abdelouas A., Moliki M.B., Magnin M., Broudic V. [in preparation]. Quantification of C-14 in liquid and gas (D3.9). *CArbon-14 Source Term – CAST*, Available from <http://www.projectcast.eu>

BARBERIS P. ET AL. [1997]. On Raman spectroscopy of zirconium oxide films. *Journal of Nuclear Materials*, Vol. 246, 232-243.

BIORAD Chelex100 and Chelex 20 Chelating Ion Exchange Resin, Instruction Manual.

BLEIER, A., BEUERLE, M., ELLINGER, M., AND BOHLEN, D. [1988]. Untersuchungen zum chemischen Status von C14 nach Auslaugung mit einer Salzlösung aus Hüllmaterial bestrahlter DWR- und SWR-Brennelemente. *Siemens, KWU*, U9 414/88/001.

BOTTOMLEY D., WEGEN. D, KNOCHE D., DE WEERD W., METZ V. [2015]. Intermediate report on the analysis of samples total C14 content (D3.6). *CArbon-14 Source Term – CAST*, Available from <http://www.projectcast.eu>.

CARON N., VEILLER L., BUCUR C., FULGER M. JOBBAGY V., TANABE H., SAKURAGI T., BOTTOMLEY D. [2014]. Definition of operating conditions and presentation of the leaching experiments (D3.2). *CArbon-14 Source Term – CAST*, Available from <http://www.projectcast.eu>.

CHANDA M., ODRISCOLL K., REMPEL G. [1988]. Ligand exchange sorption of arsenate and arsenite anions by chelating resins in ferric ion form: II. Iminodiacetic chelating resin Chelex 100. *Reactive Polymers, Ion Exchangers, Sorbents*. Vol. 8 (1) p85–95.

COLLINS J. L., EGAN B. Z., ANDERSON K. K., CHASE C. W., MROCHEK J. E., BELL J. T., JERNIGAN G. E. [1995]. Evaluation of selected ion exchangers for the removal of cesium from MVST W-25 supernate. Oak Ridge National Lab., TN (United States). Funding organisation: USDOE, Washington, DC (United States), ORNUTM-12938, p60.

FEDERATION OF ELECTRIC POWER COMPANIES (FEPC) AND JAPAN ATOMIC ENERGY AGENCY (JAEA). [2007]. Second progress report on research and development for TRU waste disposal in Japan.

FILELLA M., BELZILE N., CHEN Y. W. [2002]. Antimony in the environment: a review focused on natural waters II. Relevant solution chemistry. *Earth-Science Reviews* Vol.59, p265–285.

FILELLA M., MAY P. M. [2003]. Computer simulation of the low-molecular-weight inorganic species distribution of antimony(III) and antimony(V) in natural waters. *Geochimica et Cosmochimica Acta*. Vol. 67, No. 21, p4013–403.

GRAS J.M, [2014]. State of the art of ¹⁴C in Zircaloy and Zr alloys – C-14 release from zirconium alloy hulls (D3.1). *CArbon-14 Source Term – CAST*, Available from <http://www.projectcast.eu>.

HEIKOLA T. [2014]. Leaching of C-14 in repository conditions. Transport and speciation. *Vtt - Julkaisija - Utgivare*. 157.

HERM, M., GONZÁLEZ-ROBLES, E., BÖTTLE, M., MÜLLER, N., PAPAIOANNOU, D., WEGEN, D. H., DAGAN, R., KIENZLER, B., AND METZ, V. [2015-a]. Description of Zircaloy-4 dissolution experiment in a shielded box (D3.8). *CArbon-14 Source Term – CAST*, Available from <http://www.projectcast.eu/cms-file/get/iFileId/2493>.

HERM, M. [2015-b]. Study on the effect of speciation on radionuclide mobilization – C-14 speciation in irradiated Zircaloy-4 cladding and nitrate/chloride interaction with An(III)/Ln(III). Karlsruhe Institute of Technology (KIT). Available from <http://dx.doi.org/10.5445/IR/1000051441>.

HILLNER, E. [1977]. Corrosion of zirconium-base alloys—An overview. *Zirconium in the Nuclear Industry, 3rd Int. Symp., ASTM STP, Vol. 633*, 211-235.

JOBAGY V., DRUYTS F., TANABE H., BOTTOMLEY D. [2014]. Progress report on corrosion tests in the hot cell-experimental setup (D3.4). *CArbon-14 Source Term – CAST*, Available from <http://www.projectcast.eu>.

KAMENÍK J., DULAIIOVA H., ŠEBESTA F., & ŠŤASTNÁ K. [2012]. Fast concentration of dissolved forms of cesium radioisotopes from large seawater samples. *J Radioanal Nucl Chem*. DOI 10.1007/s10967-012-2007-4.

MIMURA H., LEHTO J., HARJULA R. [1997]. Chemical and Thermal Stability of Potassium Nickel Hexacyanoferrate (II), *Journal of Nuclear Science and Technology*, Vol.34:6, p582–587.

NECIB S., BOTTOMLEY D., ALI BAHRI M., BUCUR C., CARON N., COCHIN F., FULGER M., HERM M., JOBAGY V., KASPRZAK L., LEGAND S., MAGNIN M., METZ V., SAKURAGI T., SUZUKI T., TANABE H.[2015]. 2nd year Annual WP3 progress report (D3.11). *CArbon-14 Source Term – CAST*, Available from <http://www.projectcast.eu/cms-file/get/iFileId/2493>.

NEEB, K. H. [1997]. *The radiochemistry of nuclear power plants with light water reactors* (Berlin: de Gruyter).

PAI S.-C. [1988-a]. Pre-concentration efficiency of chelex-100 resin for heavy metals in seawater : Part 2. Distribution of Heavy Metals on a Chelex-100 Column and Optimization

of the Column Efficiency by a Plate Simulation Method. *Analytica Chimica Acta*. Vol. 211 p271–280.

PAI S.-C., WHUNG P.-Y., LAI R.-L. [1988-b]. Pre-concentration efficiency of chelex-100 resin for heavy metals in seawater : Part 1. Effects of pH and Salts on the Distribution Ratios of Heavy Metals. *Analytica Chimica Acta*. Vol. 211 p257–270.

PAKALNS P. [1980]. Separation of uranium from natural waters on chelex-100 resin. *Analytica Chimica Acta*. 120, p289–296.

PITMAN A.L., POURBAIX M., DE ZOUBOV N. [1957]. Potential-pH diagram of the antimony–water system. Its applications to properties of the metal, its compounds, its corrosion, and antimony electrodes. *J. Electrochem. Soc.* 104, p594–600.

SAKURAGI, T., YAMASHITA, Y., AKAGI, M., and TAKAHASHI, Y. [2016]. Carbon 14 distribution in irradiated BWR fuel cladding and released carbon 14 after aqueous immersion of 6.5 years, *Procedia Chemistry, Proceedings of the 5th International ATALANTE Conference on Nuclear Chemistry for Sustainable Fuel Cycles*. (in Press).

SAKURAGI, T., TANABE, H., HIROSE, E., SAKASHITA, A., and NISHIMURA, T. [2013]. Estimation of carbon 14 inventory in hull and end-piece wastes from Japanese commercial reprocessing operation. *Proc. 15th International Conference on Environmental Remediation and Radioactive Waste Management, ICEM2013*, Brussels, Belgium.

SASOH M. [2008]. The study of the chemical forms of C-14 released from activated metals, pp. 19-21 in NAGRA Working Report NAB 08-22.

SCHUMANN, D., STOWASSER, T., VOLMERT, B., GÜNTHER-LEOPOLD, I., LINDER, H. P., AND WIELAND, E. [2014]. Determination of the ¹⁴C Content in Activated Steel Components from a Neutron Spallation Source and a Nuclear Power Plant. *Anal. Chem.*, Vol. 86, 5448-5454.

TAKAHASHI R., SASOH M., YAMASHITA Y., TANABE H., SAKURAGI T. [2013]. Improvement of inventory and leaching rate measurements of C-14 in hull waste, and separation of organic compounds for chemical species identification, paper (draft) presented at MRS 2013.

TAKENO N. [2005]. Atlas of Eh-pH diagrams, Intercomparison of thermodynamic databases, Geological Survey of Japan Open File Report No.419, National Institute of Advanced Industrial Science and Technology, May 2005.

VERLET R. [2015]. Influence de l'irradiation et de la radiolyse sur la vitesse et les mécanismes de corrosion des alliages de zirconium. École Nationale Supérieure des Mines de Saint-Étienne.

YAMAGUCHI R. ET AL. [1999]. A study on chemical forms and migration behavior of radionuclides in hull wastes. *Radioactive Waste Management and Environmental Remediation*, ASME 1999.

YAMASHITA, Y., TANABE, H., SAKURAGI, T., TAKAHASHI, Y., AND SASOH, M. [2014]. C-14 release behavior and chemical species from irradiated hull waste under geological disposal conditions, *Mater. Res. Soc. Symp. Proc.*, Vol. 1665, 187-194.

Glossary

AMS: Accelerated Mass Spectrometer

Département de traitement et de conditionnement des déchets/Scanning electroChemical Microscopy/Laboratoire de Modélisation des Plasmas Astrophysique (DTCD/SECM/LMPA)

BWR: Boiling Water Reactor

GC: Gas Chromatography

GMS: Gas Mass spectrometer

HLPC: High Performance Liquid Chromatography

IC: Ion Chromatography

ICP-MS: Inductively coupled plasma mass spectrometry

IR: Infra-Red Spectroscopy

LASE: Laboratoire d'Analyses en Soutien aux Exploitants

LRMO: Laboratoire de Radiolyse et de la Matière Organique

LPR : Linear Polarisation Resistance

LSC: Liquid Scintillation Counting

OM: Optical Microscopy

PWR: Pressurised Water Reactor

SEM: Scanning Electron Microscopy

Zry-2, Zr-2: Zircaloy-2

Zry-4, Zr-4: Zircaloy-4